

This pdf file consists of all figures contained in:

CONVERGENT AND COLLISIONAL TECTONICS IN PARTS OF OREGON,
MAINE, AND THE VERMONT- QUEBEC BORDER

by

Adam Schoonmaker

A Dissertation

Submitted to the University at Albany, State University of New York

in Partial Fulfillment of

the Requirements for the Degree of

Doctor of Philosophy

College of Arts and Sciences

Department of Earth and Atmospheric Sciences

2005

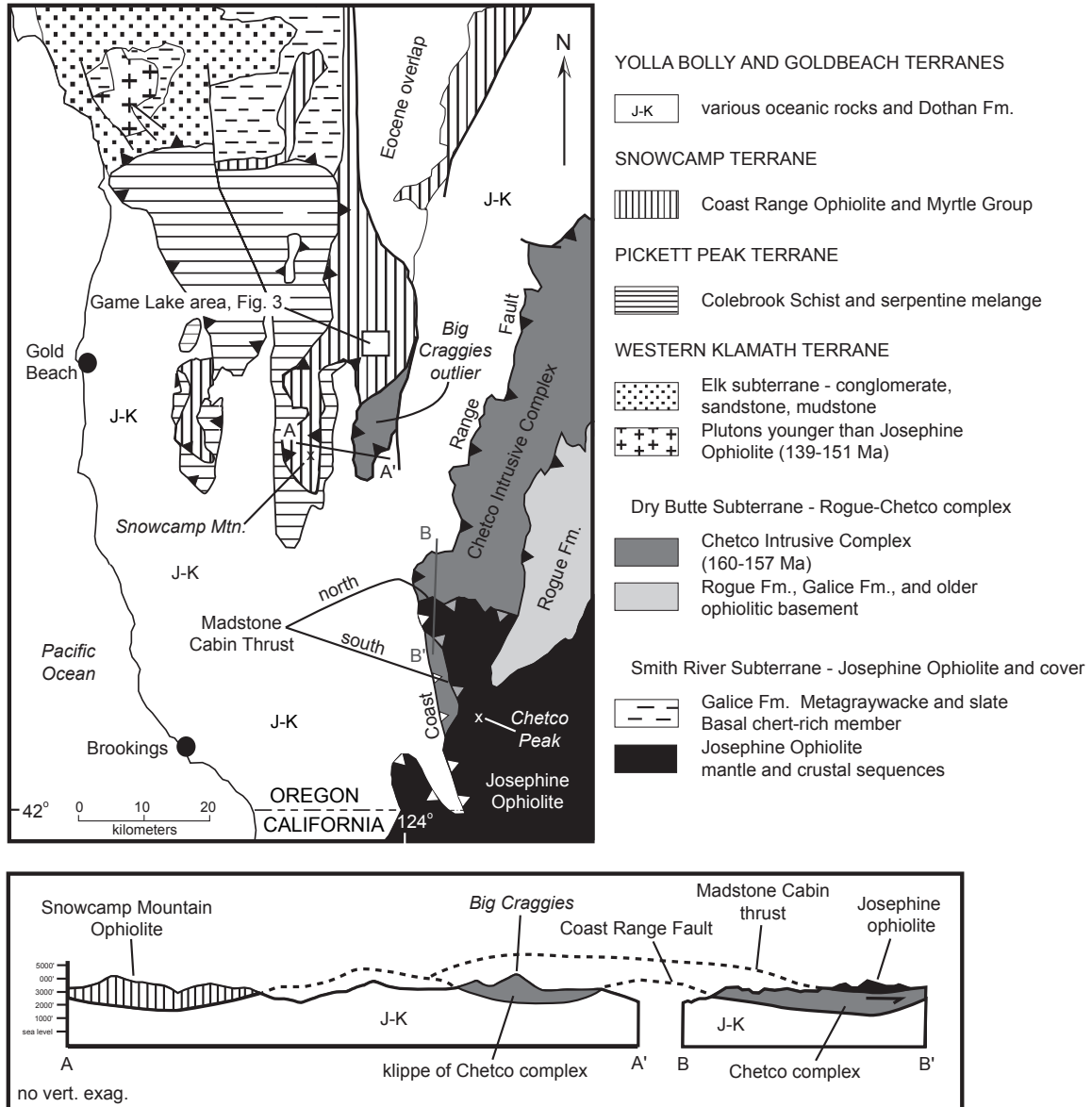


Figure 1. Regional geologic map and schematic cross-sections across the Snowcamp terrane (A-A') and the Madstone Cabin thrust (B-B').

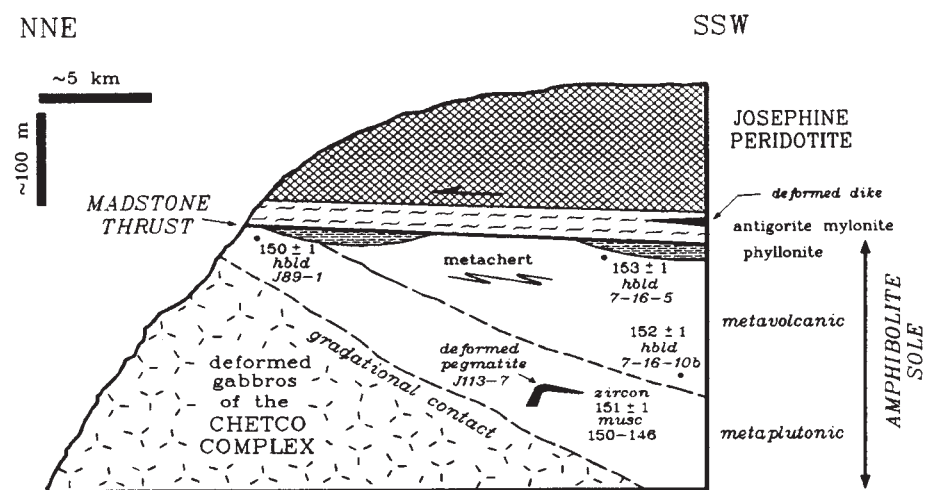


Figure 2. Schematic cross-section of the Madstone Cabin thrust (from Harper et al. 1996).

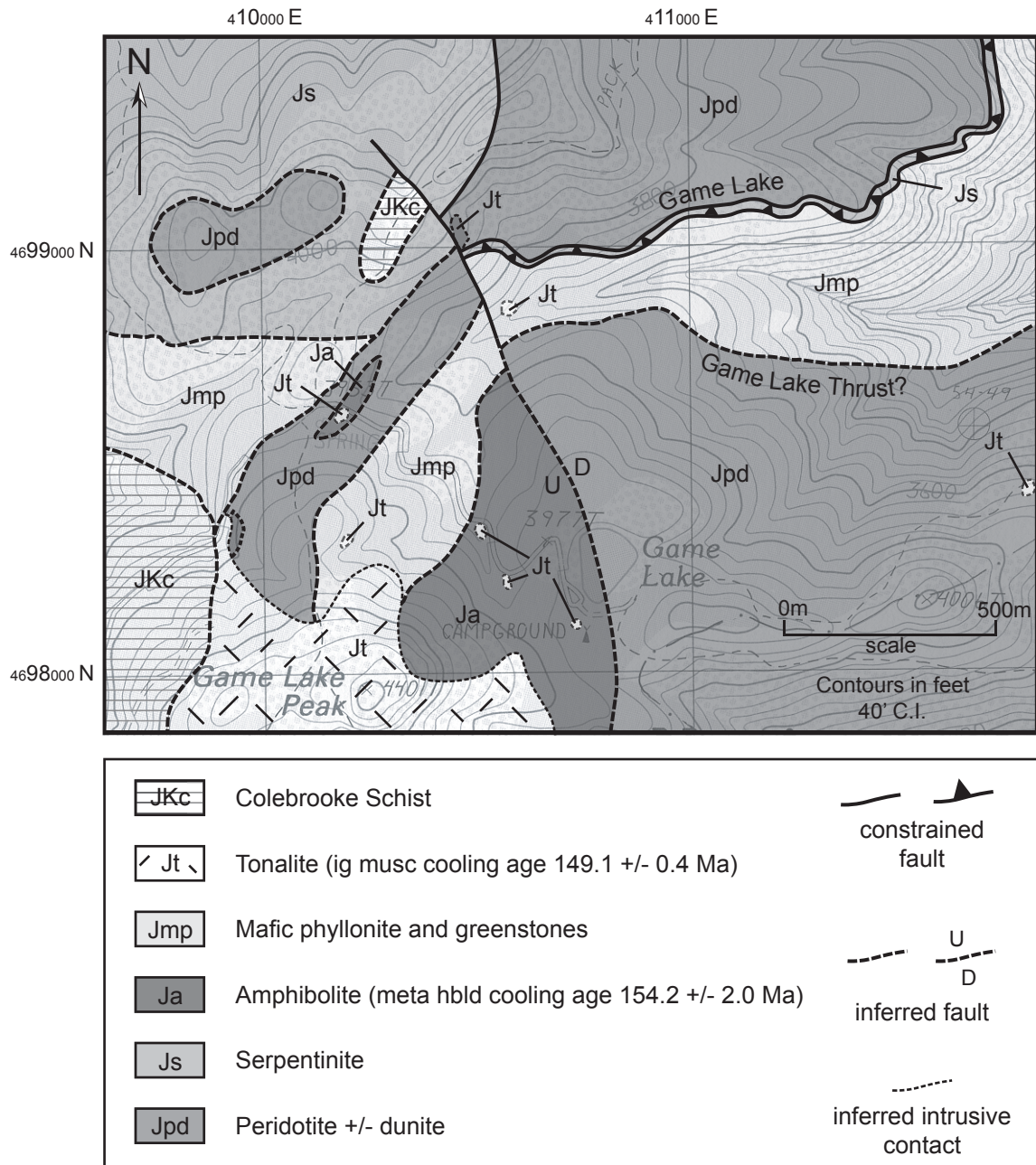


Figure 3. Geologic Map of the Game Lake area. Base from Horesign Butte 7.5' USGS topographic quadrangle.

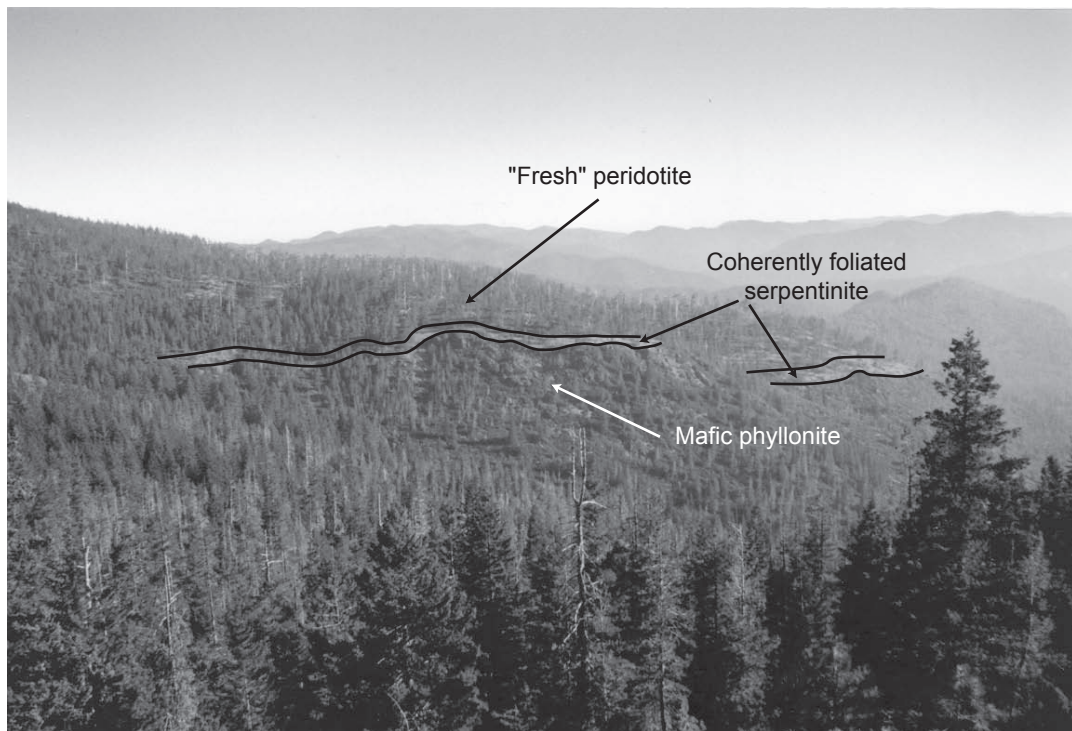


Figure 4. View of the Game Lake thrust (looking approximately north).

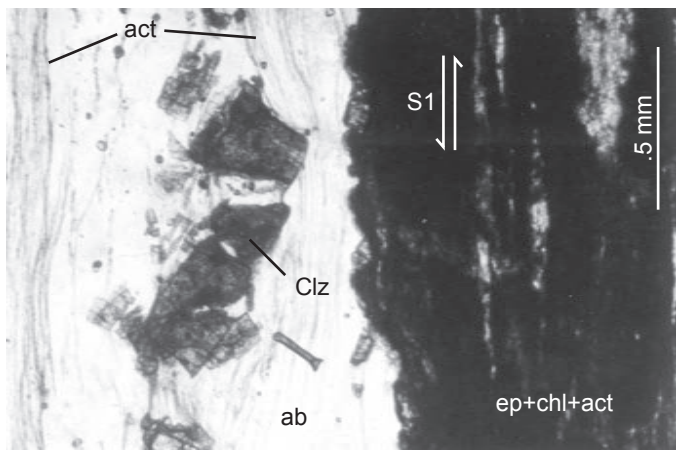


Figure 5. Plane light (2.5x) photomicrograph of mylonitic texture of mafic phyllonite (BC-307). Note imbricated and rotated porphyroclasts of clinozoisite (clz) and fibrous actinolite (act). Light-colored albite-rich zone (ab) shows strong foliation (S1) while foliation is dark area is partly obscured by non-foliated chlorite (chl) and epidote (ep).

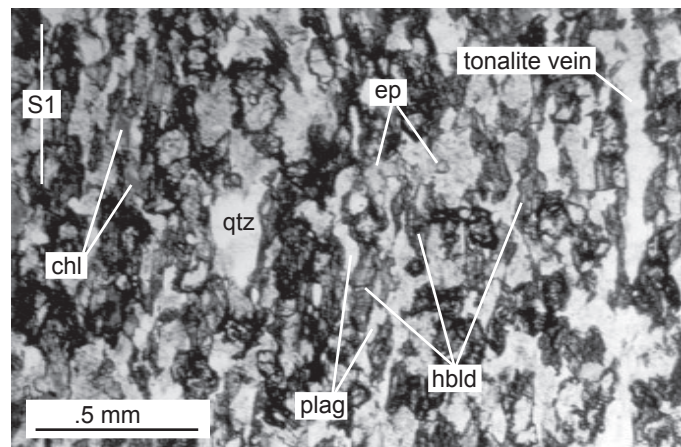


Figure 6. Plane light (2.5x) photomicrograph of amphibolite (BC-136). Foliation (S1) defined by hornblende (hbld) and plagioclase (plag) and to a lesser extent by epidote (ep) and quartz (qtz). Slight alteration of hornblende to chlorite (chl) is present. Tonalite vein is deformed parallel to foliation.

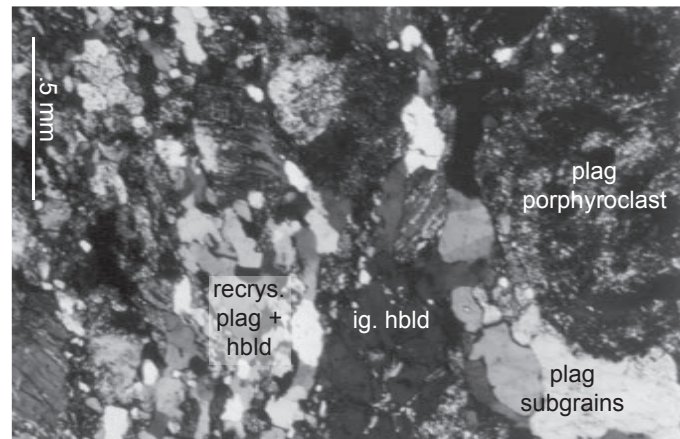


Figure 7. Crossed-nicols (2.5x) photomicrograph of metagabbro (BC-005) showing protomylonitic texture. Large igneous plagioclase (plag) porphyroclasts show significant sausseritization and subgrain development (lower right). Small, oriented, recrystallized grains of hornblende (hbld) and plagioclase define foliation.

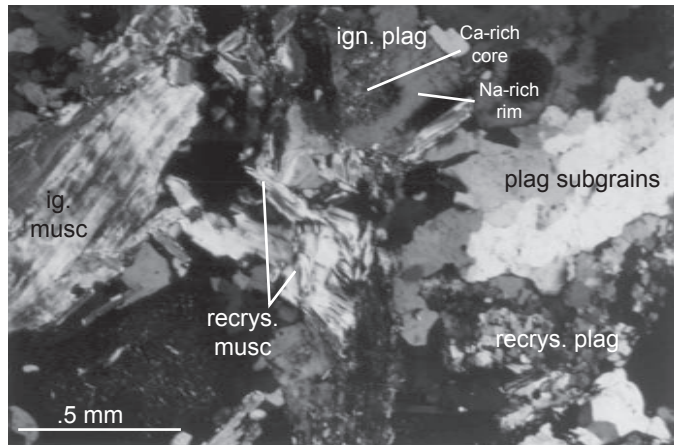


Figure 8. Crossed-nicols (2.5x) photomicrograph of tonalite (BC-133). Large igneous muscovite (musc) is strained rimmed by fine-grained recrystallized muscovite. Present are large igneous plagioclase (plag), small recrystallized plagioclase, and subgrains.



Figure 9. Field photograph of amphibolite (BC-037) with folded tonalite dikelet that parallels S_1 amphibolitic foliation. Pencil is 14 cm long.



Figure 10. Field photograph of open fold in amphibolite (BC-136). Dog head is 14 cm wide.

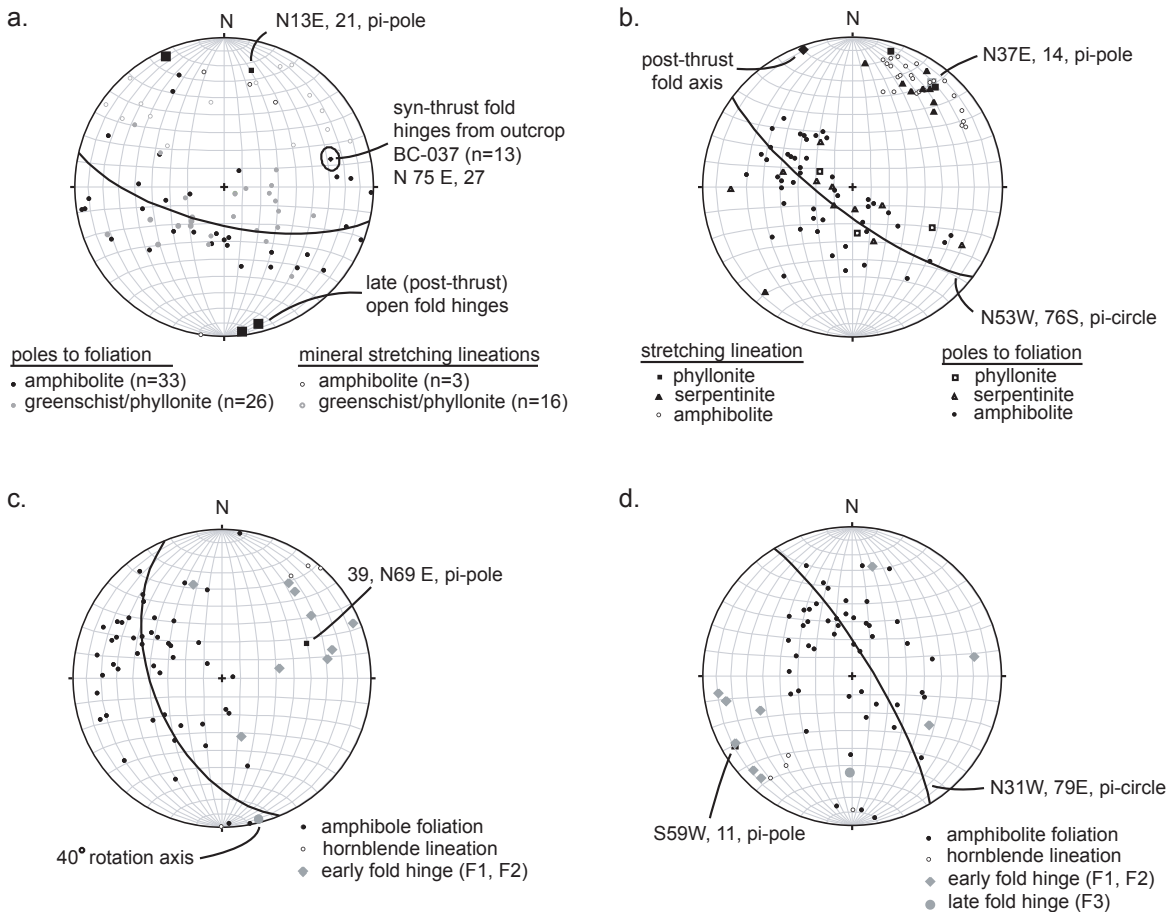


Figure 11. Structural data from Game Lake and Madstone Cabin thrusts.

a.) Structural data from Game lake area (this study). b.). Structural data from southern exposure of Madstone Cabin thrust (modified from Harper et al, 1990). c.) Rotated structural data from northern exposure of Madstone Cabin thrust (adapted from Loney and Himmelberg, 1977). d.) Unrotated structural data from northern exposure of Madstone Cabin thrust (modified from Loney and Himmelberg, 1977).

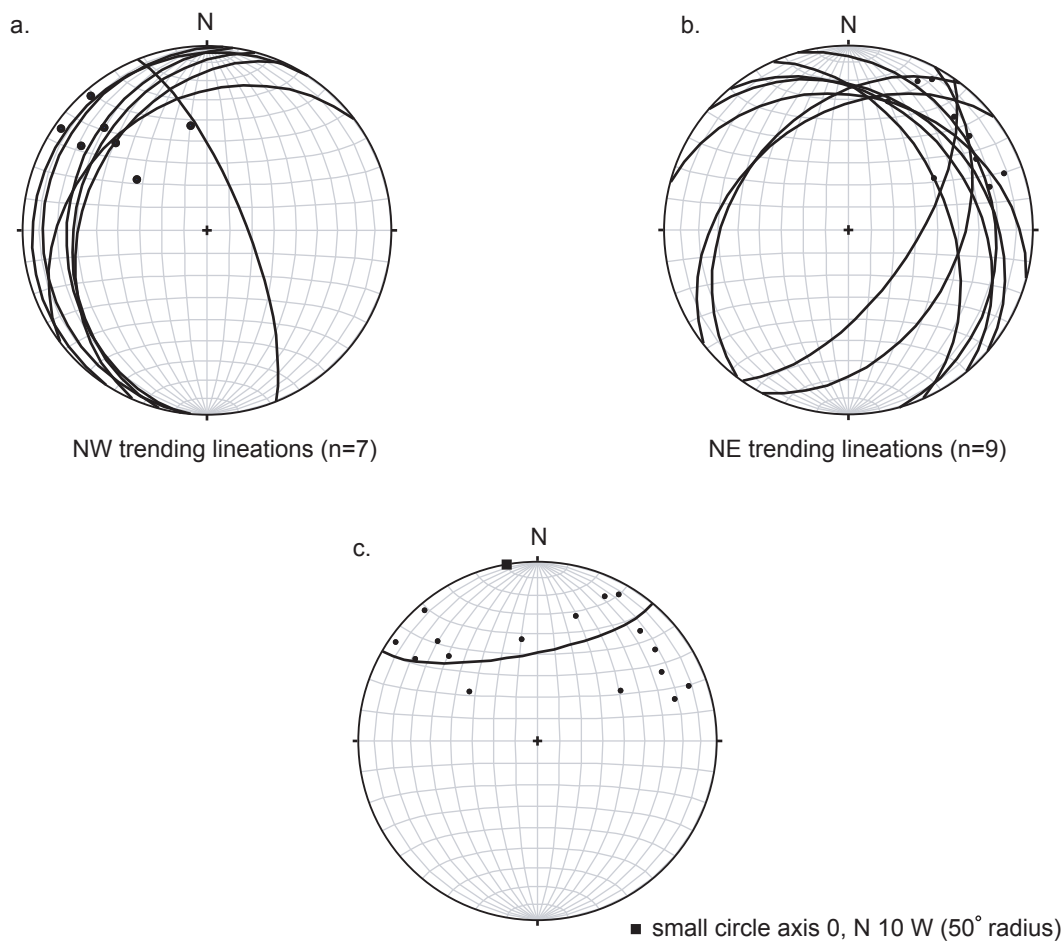


Figure 12. Lineation data from Game Lake thrust. a.) Plot of NW trending lineations and associated foliations on which they occur. b.) Plot of NE trending lineations and associated foliations. c.) Plot of NW and NE lineations scatter along a small circle whose axis approximates average late fold axis (0, N 10 W, 500 radius), suggesting conical folding.

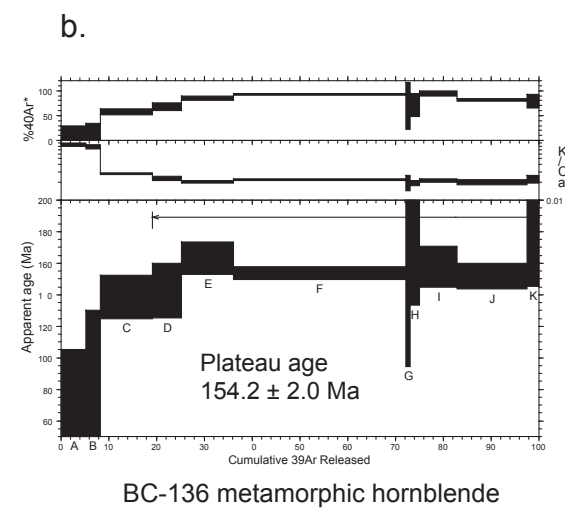
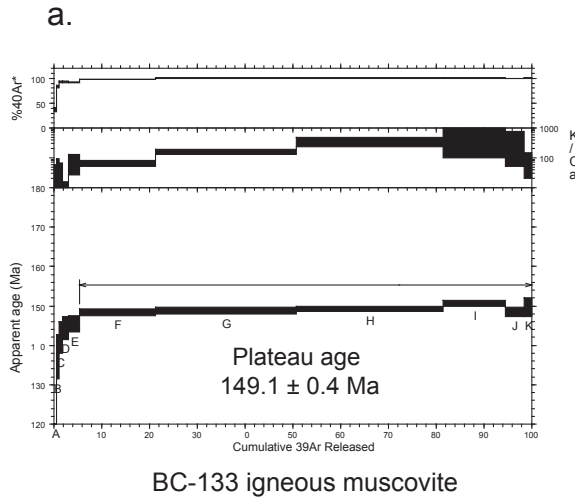


Figure 13. $40\text{Ar}/39\text{Ar}$ release spectra. a. tonalite sample BC-133 (igneous muscovite). b. amphibolite sample BC-136 (metamorphic hornblende).

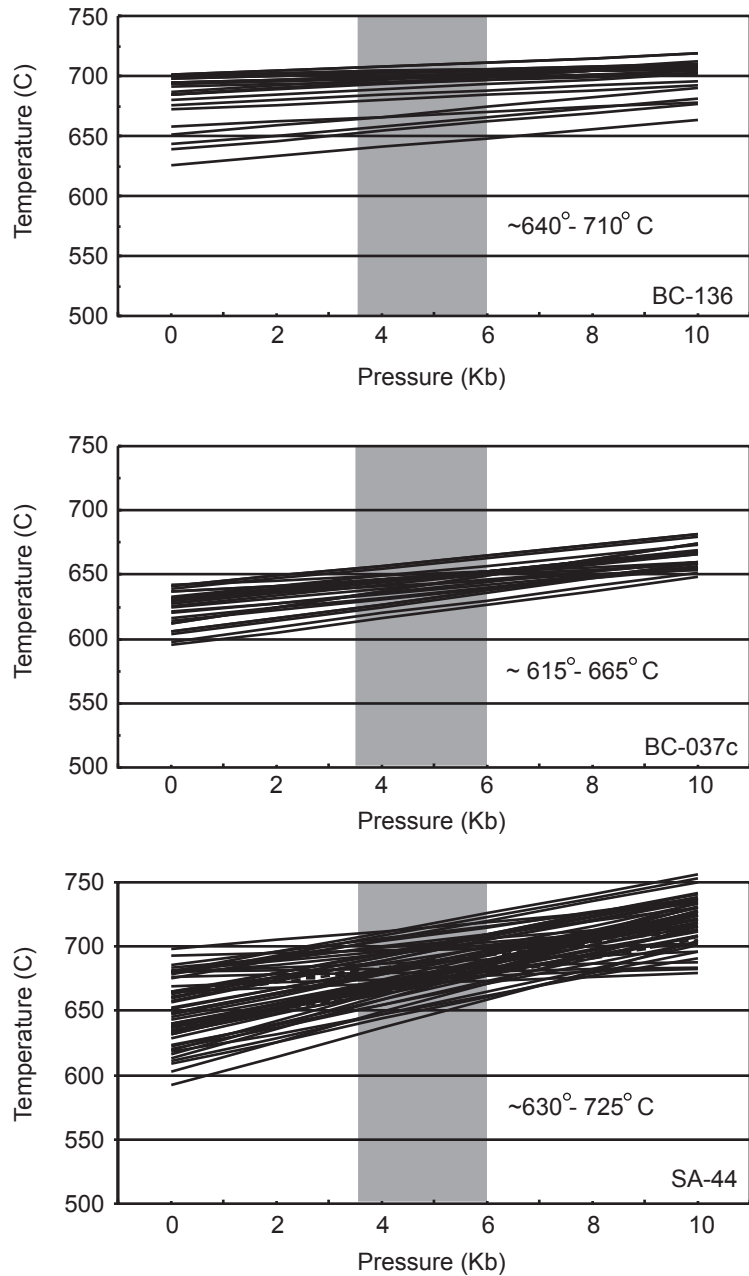
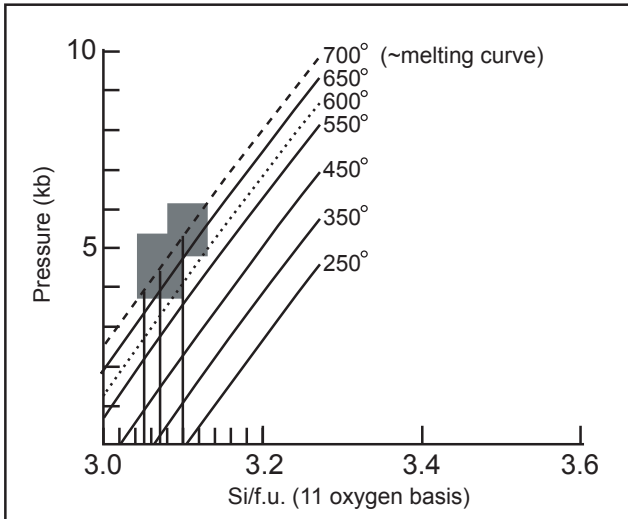


Figure 14. Results of application of geothermometer A (tremolite-richterite) of Holland and Blundy (1994) to coexisting hornblende-plagioclase pairs in amphibolites from Madstone Cabin thrust (SA-44) and Game Lake thrust (BC-136, BC-037c). Shaded areas represent pressure range derived from phengite barometer (see figure 15).

a.

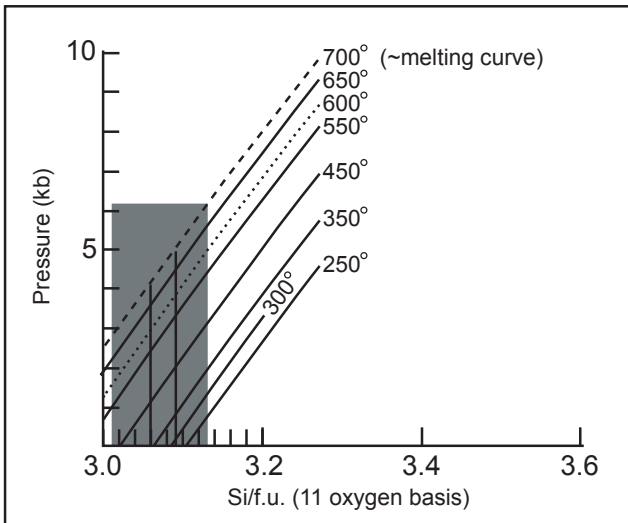


Average silica content of igneous
muscovite/sample

Madstone Cabin Thrust:
Si = 3.07 J82-3 (ign.) n = 13

Game Lake Thrust:
Si = 3.10 BC-133 (ign.) n = 5
Si = 3.05 BC-123 (ign.) n = 7

b.



Average silica content of metamorphic
muscovite/sample

Madstone Cabin Thrust:
Si = 3.09 J82-3 (meta.) n = 11

Game Lake Thrust:
Si = 3.06 BC-133 (meta.) n = 6
Si = 3.06 BC-123 (meta.) n = 6

Figure 15. Results of application of phengite geobarometer of Massone and Schreyer (1987) to igneous (a.) and metamorphic (b.) muscovite in tonalites from Madstone Cabin thrust (J82-3) and Game Lake thrust (BC-123, BC-133). Vertical bars represent average silica content of igneous and metamorphic muscovite from each sample. Shaded area represents the range of all analyses for each sample using constraints given in text.

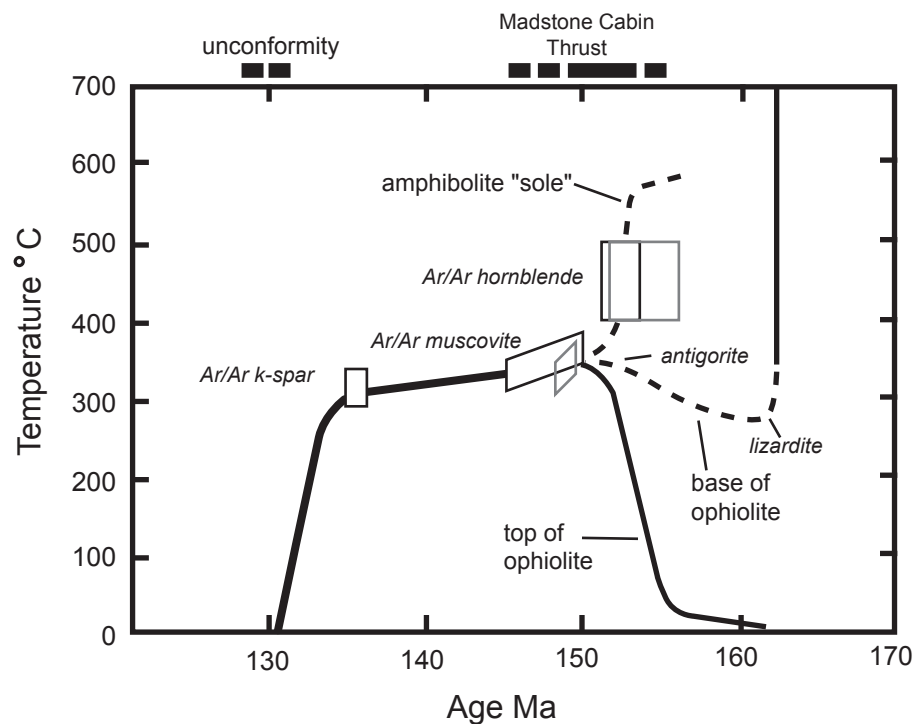


Figure 16. T-t path for Madstone Cabin and Game Lake thrusts. Black lines and boxes (Madstone Cabin thrust) modified from Harper et al. (1996). Gray boxes represent T-t data ($^{40}\text{Ar}/^{39}\text{Ar}$ ages and closure temperature ranges) from Game Lake thrust.

1a.	Game Lake thrust (this study)	Madstone Cabin thrust (Harper et al., 1990; 1994 1996; Loney and Himmelberg, 1977)	Ib.	Coast Range Ophiolite (Shervais, 1990; Hopson, 1981; Hopson et al. 1996; Shervais et al., 2004)	Josephine Ophiolite (Loney and Himmelberg, 1997; Saleaby et al., 1982; Pessagno and Blome, 1990; Harper et al., 1994; Palfy et al. 2000; Harper, 2003)
Similarities:				Overlying cover:	
Lithic units	-peridotite and dunite -coherent basal serpentinite -mafic phyllonite -amphibolite -syntectonic mu-gt tonalite	-harzburgite and dunite -basal serpentinite mylonite -mafic phyllonite -amphibolite -syntectonic mu-gt tonalite	Great Valley Group	Myrtle Group	
Structures	-NE trending early, tight to isoclinal folds -NE trend of π -pole to amphibolite and mafic phyllonite foliations -NE and NW trending lineations -NE transport direction of upper block (modern coordinates) -late open folds	-NE trending early, tight to isoclinal folds -NE trend of π -pole to amphibolite and mafic phyllonite foliations -NE trending lineation -NE transport direction of upper block (modern coordinates) -late open folds	Continuous sedimentation during the Nevadan Orogeny	Unconformity (Nevadan Orogeny)	
Cooling ages: amphibolite	154.2 ± 2.0 Ma ($^{40}\text{Ar}/^{39}\text{Ar}$ hblld, 1-sigma)	150.3 ± 1.0 Ma ($^{40}\text{Ar}/^{39}\text{Ar}$, hblld, 1-sigma)	Volcaniclasts and chert (Oxfordian – Tithonian)	Galice Flysch (Kimmeridgian) Hemipelagic sequence (Oxfordian or Bathonian)	
syntectonic tonalite	149.1 ± 0.4 Ma ($^{40}\text{Ar}/^{39}\text{Ar}$, musc, 1-sigma)	150 to 146 Ma ($^{40}\text{Ar}/^{39}\text{Ar}$, musc, 1-sigma)	Crustal sequence:	Crustal sequence:	
Metamorphic history	prograde amphibolite facies 550° to $>600^\circ\text{C}$, 3.5 - 6 kb	550° - $>600^\circ\text{C}$, 3.5 - 5 kb (this study) 400° to 540°C , 5.5 kb retrograde greenschist facies 0 - 6 kb (this study)	Chert interlayered with basalt (Bathonian to Early Kimmeridgian)	Tuffaceous chert between volcanic flows (Late Callovian or Bajocian)	
Differences:	Basal serpentinite composition Thickness of mafic phyllonite	Chrysotile and lizardite >100 meters	Lizardite overprinted by antigorite+brucite discontinuous	Subjacent rocks: Franciscan Complex Rogue – Chetco Arc Complex	

Table 1. (a.) Summary of characteristics of Game Lake and Madstone Cabin thrusts. (b.) Summary of significant features of the Josephine and Coast Range Ophiolites.

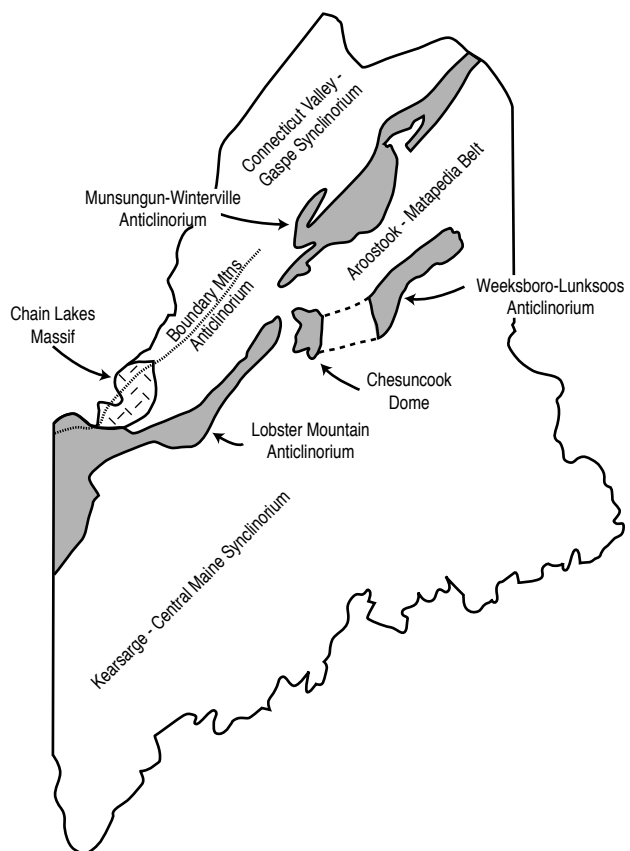


Figure 1. Generalized map showing major structures exposing pre-Silurian rocks of north-central Maine. Adapted from Osberg et al., 1985.

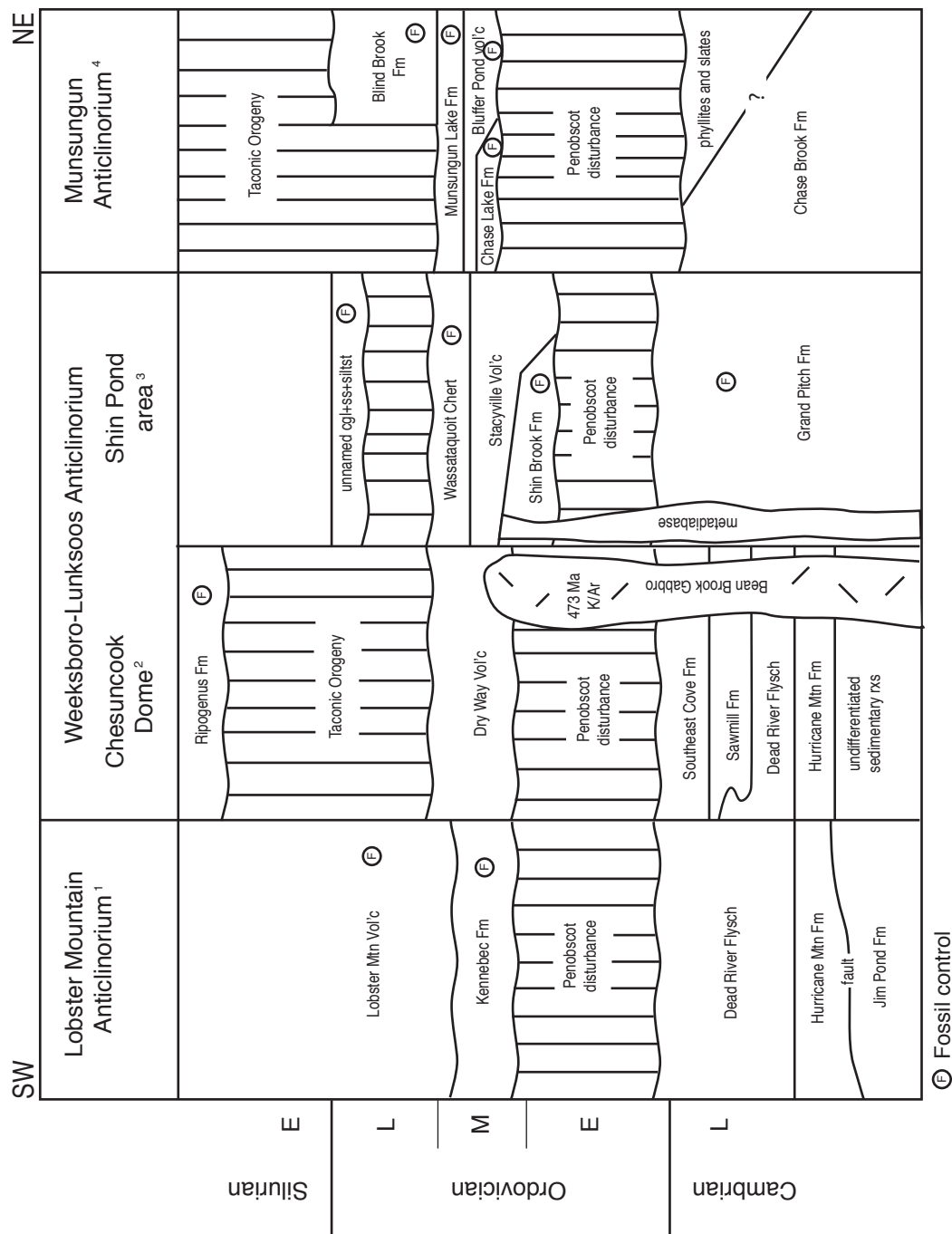
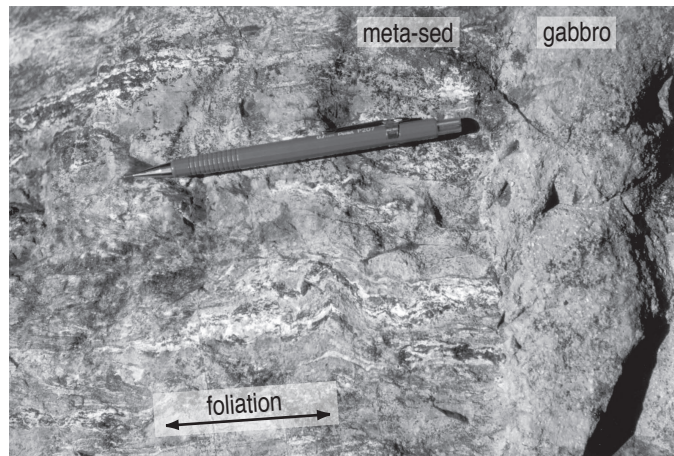
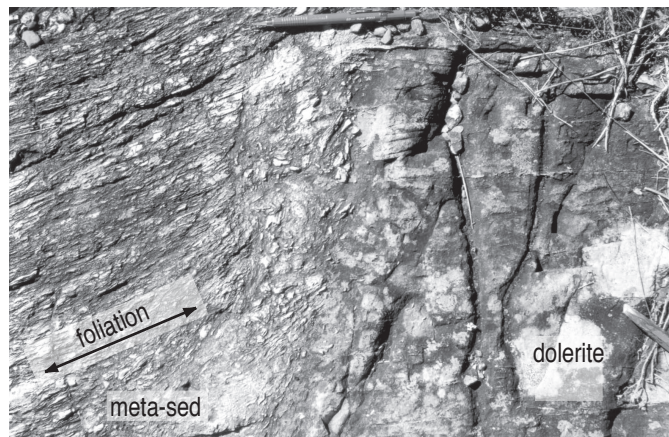


Figure 2. Correlation chart of Silurian and older rocks of north-Central Maine. Compiled from: (1) Boone and Boudette (1989), Boone et al. (1989), Boucot (1969), and Simmons Major (1988); (2) This study, Griscom (1976), Jarhling (1981, cited in Boone and Boudette, 1989), and Osberg et al. (1985); (3) Neuman (1967); 4Hall (1970).



a.



b.



c.

Figure 3. Field relations of Bean Brook Gabbro/dolerite and Cambrian(?) sedimentary rocks. a) gabbro (CSP-010b) and Hurricane Mountain Formation. b) dolerite (CSP-010d) and Hurricane Mountain Formation. c) dolerite (near CSP-009) and Dead River Flysch.

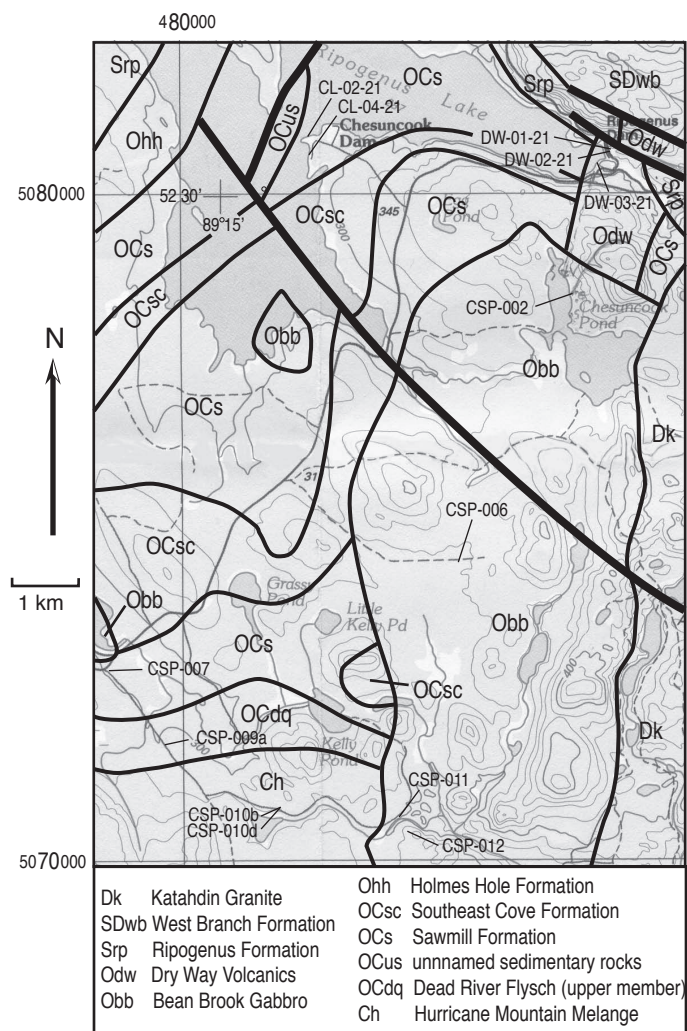


Figure 4. Geologic map of the part of the Chesuncook Dome and sample locations. Adapted from Osberg et al., 1985. Chesuncook Dam, discussed in the text, is not represented above.

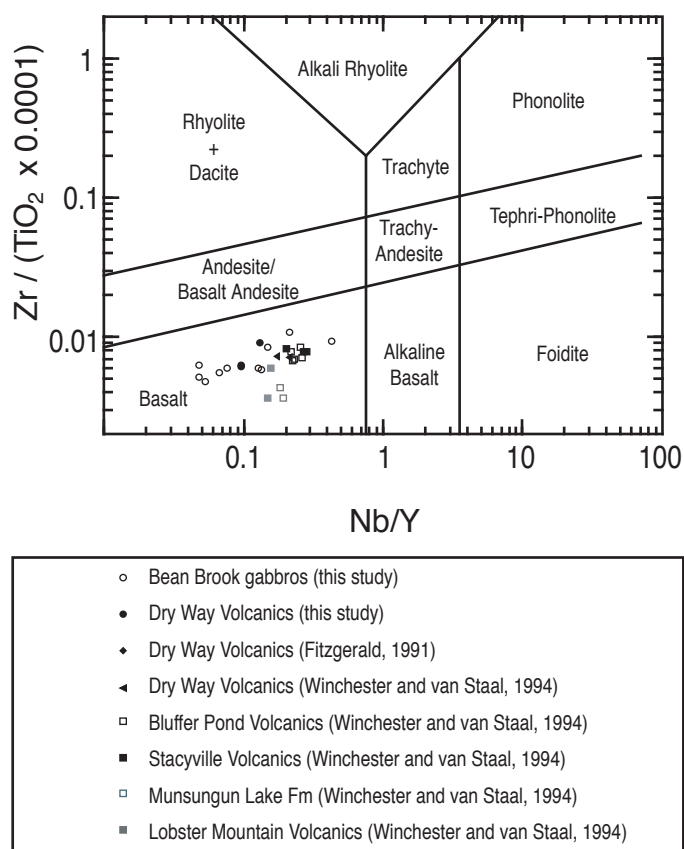
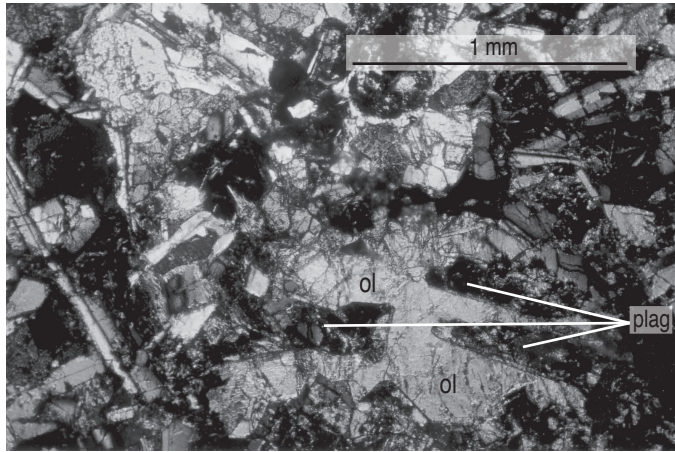
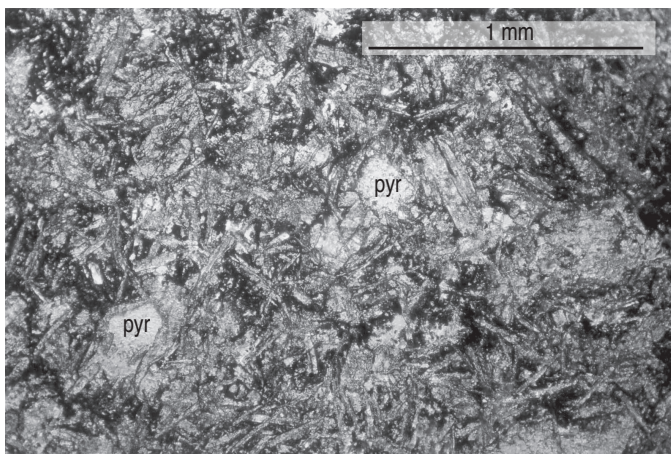


Figure 5. Rock classification diagram of Winchester and Floyd (1977), modified by Pearce (1996).



a.



b.

Figure 6. Photomicrograph of Dry Way Volcanic igneous textures. a) DW-01-21, Intergranular texture (crossed nicols, 3.5x). b) DW-03-21, radiant intergranular texture (plane light, 3.5x).

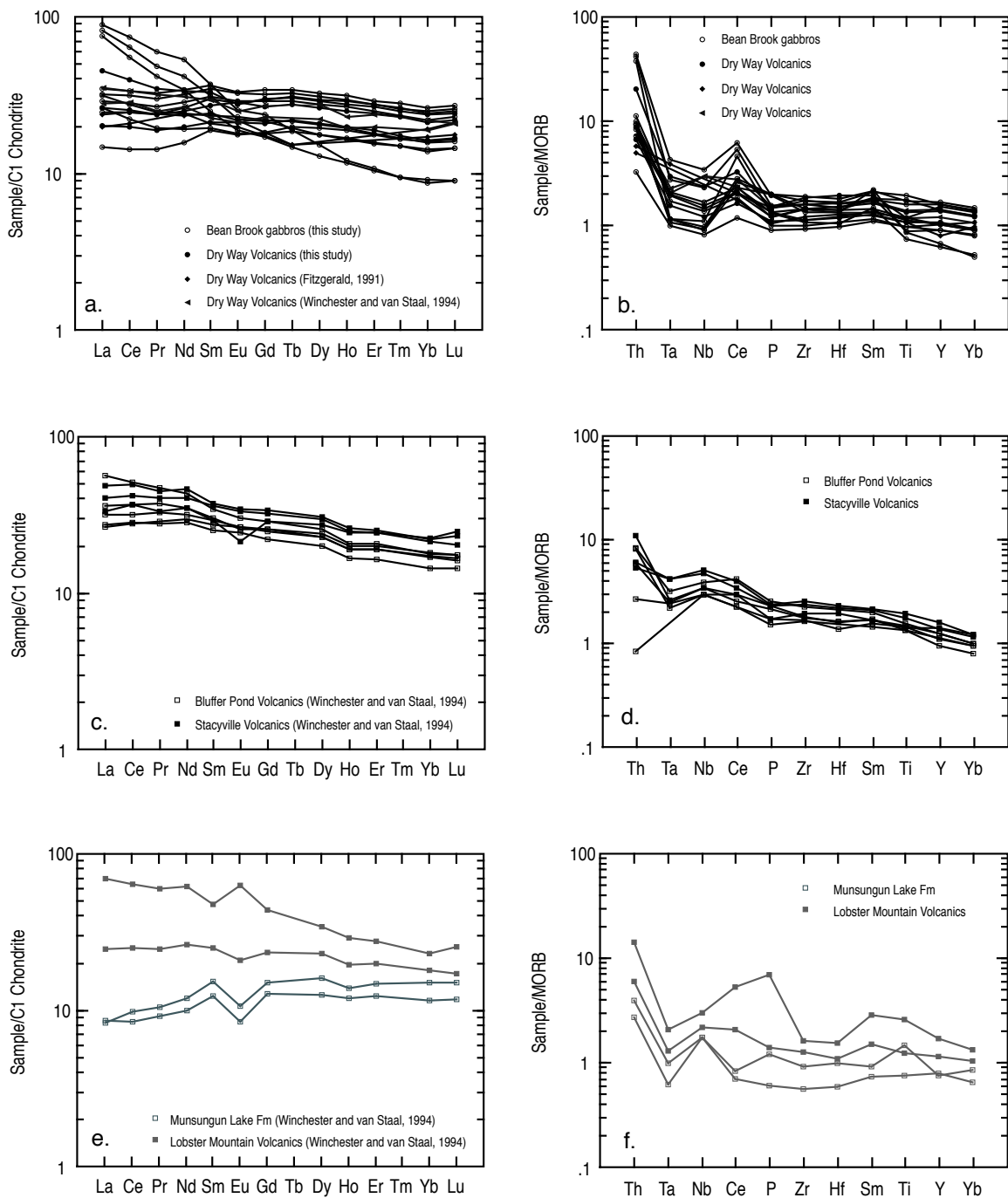


Figure 7. C1-chondrite and MORB normalized diagrams. Normalization values from Sun and McDonough (1989).

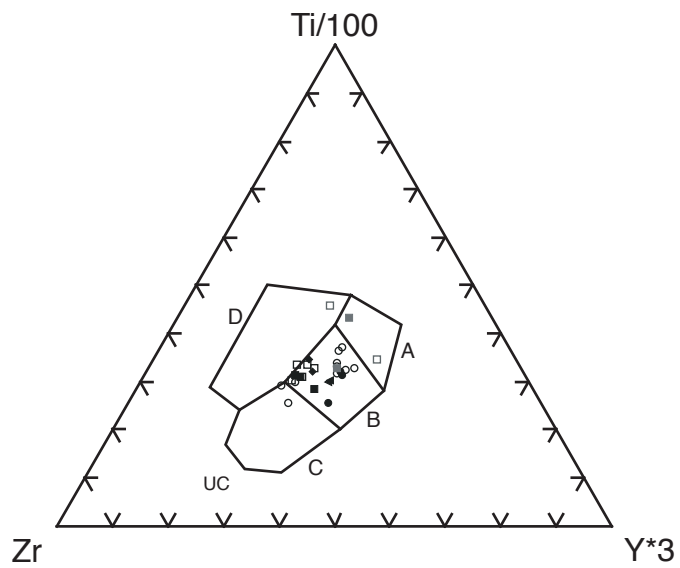


Figure 8. Ti-Zr-Y diagram of Pearce and Cann (1973). Symbols as in figure 5. UC = upper continental crust composition from McLennan (2001). Within plate basalts (oceanic and continental) plot in field D. Ocean floor basalts plot in field B. low-K tholeiites plot in fields A and B. Calc-alkaline basalts plot in field B and C.

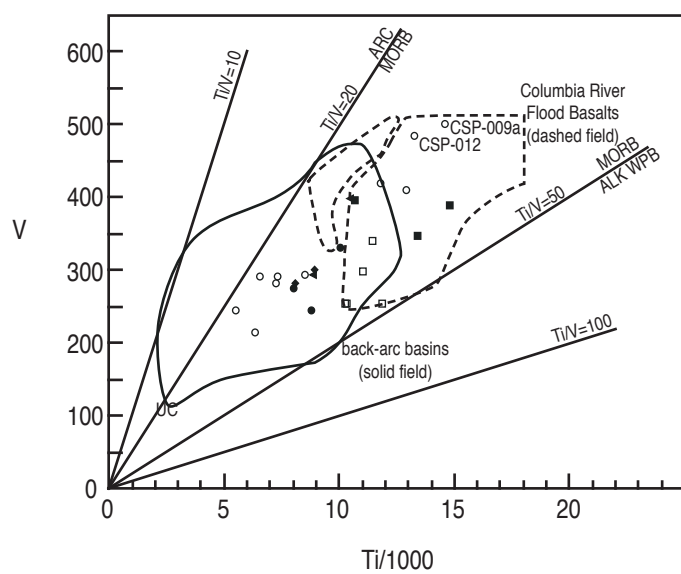


Figure 9. Ti-V diagram of Shervais (1982). Symbols as in figure 5. UC = upper continental crust composition from McLennan (2001). ARC = volcanic arc, MORB = mid-ocean ridge basalt, ALK WPB = alkaline within-plate basalt.

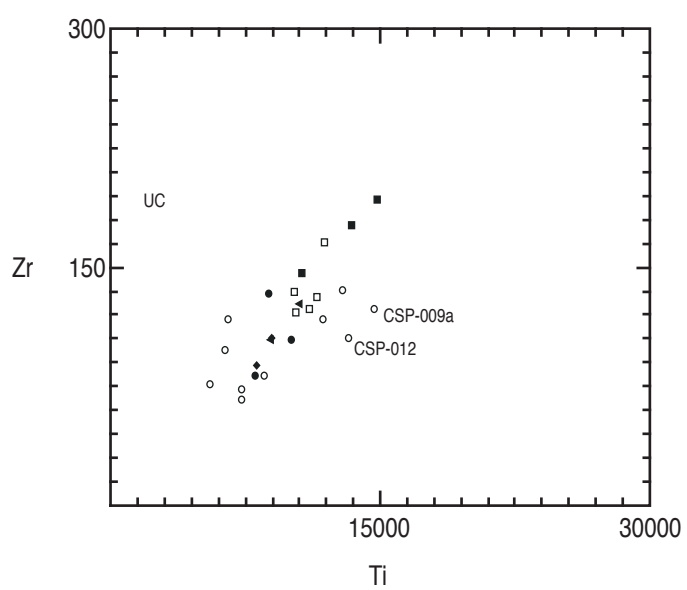


Figure 10. Ti-Zr diagram. Symbols as in Figure 5.

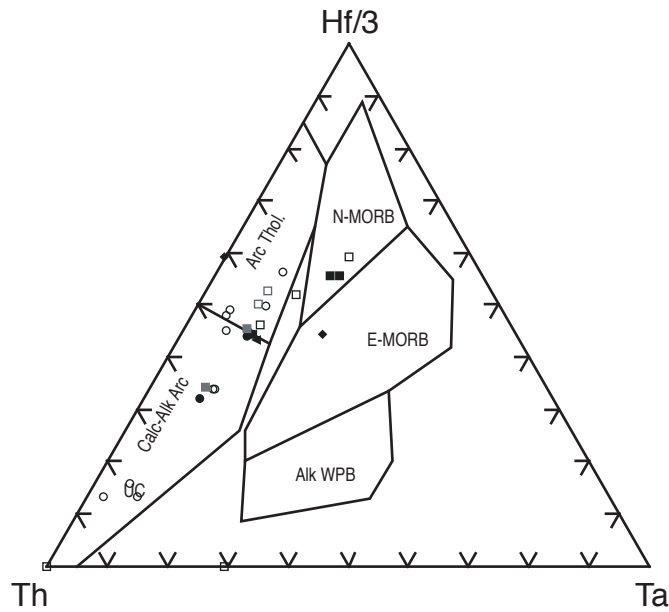


Figure 11. Th-Hf-Ta diagram of Wood (1980). Symbols as in figure 5. UC = upper continental crust composition from McLennan (2001). Calc-Alk Arc = calc-alkaline volcanic arc basalt, Arc Thol.= volcanic arc tholeiite, N-MORB = normal, depleted mid-ocean ridge basalt, E-MORB = enriched mid-ocean ridge basalt, Alk WPB = alkaline within-plate basalt.

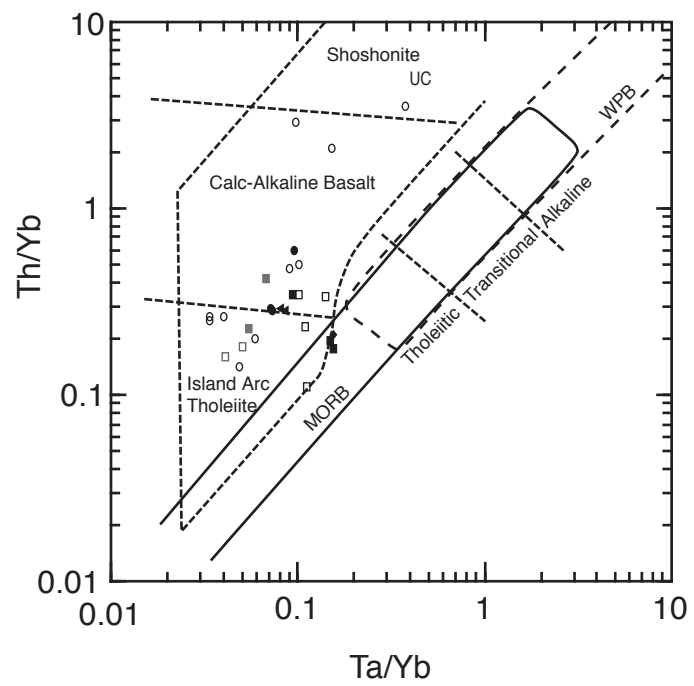


Figure 12. Th/Yb-Ta/Yb diagram of Pearce (1982). Symbols as in figure 5.
 UC = upper continental crust composition from McLennan (2001).
 MORB = mid-ocean ridge basalt, WPB = within-plate basalt.

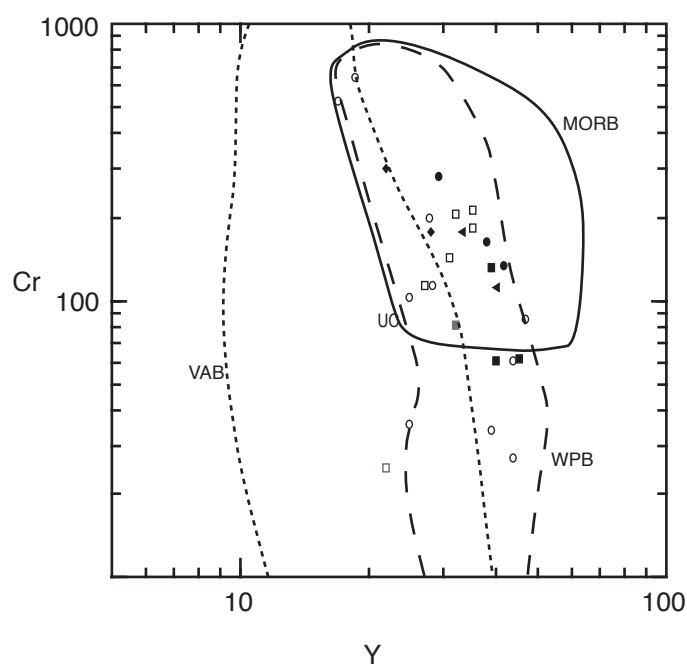


Figure 13. Cr-Y diagram of Pearce (1982). Symbols as in figure 5. UC = upper continental crust composition from McLennan (2001). VAB = volcanic arc basalt, MORB = mid-ocean ridge basalt, WPB = within-plate basalt.

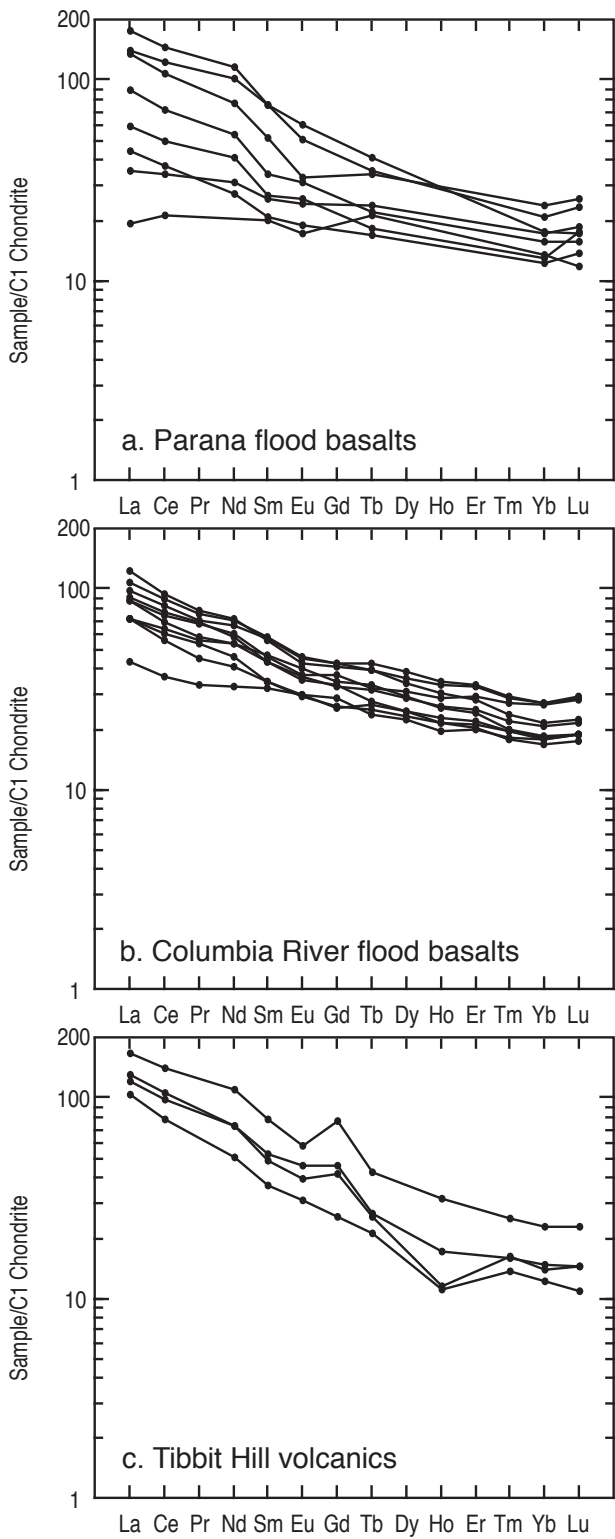


Figure 14. C1-chondrite normalized diagrams (normalization values from Sun and McDonough, 1989). a) Paraná flood basalts from Peate, 1997. b) Columbia River flood basalts from Hooper and Hawkesworth, 1993. c) Tibbit Hill volcanics from Colpron, 1990.

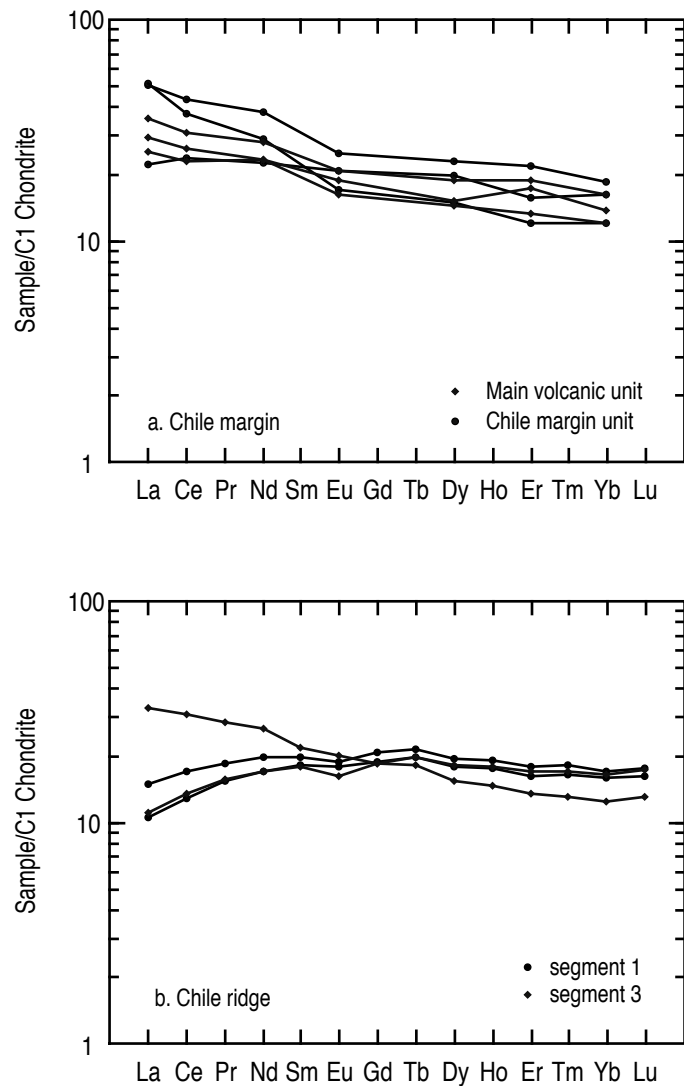


Figure 15. C1-chondrite normalized diagrams (normalization values from Sun and McDonough, 1989) of basalts from the Chile Ridge–Trench interaction. a) Chile margin basalts from Le Moigne et al., 1996. b) Chile Ridge segments from Klein and Karsten (1995).

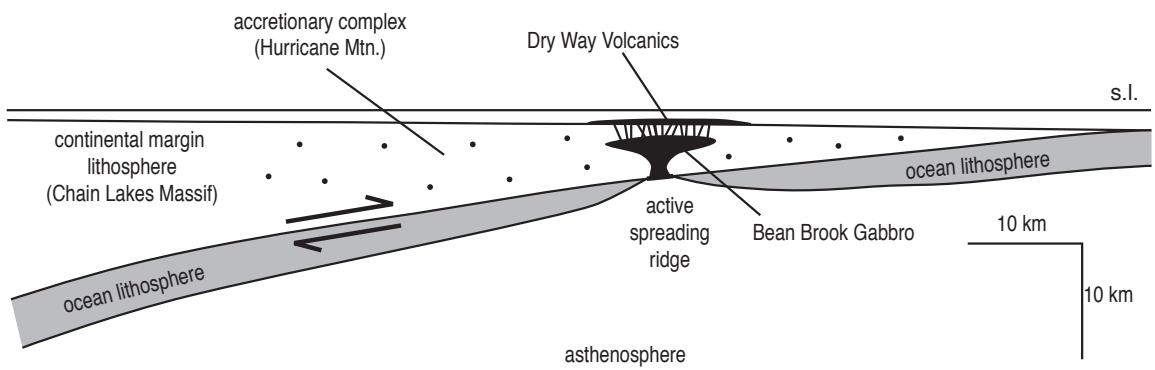


Figure 16. Schematic cartoon illustrating Ordovician ridge subduction beneath Chain Lakes Massif.

Sample #s	Dry Way Volcanics				Bean Brook Gabbro				'Boom House'					
	DW 01-21	DW 02-21	DW 03-21	CSP 002	CSP 006	CSP 007	CSP 009a	CSP 010b	CSP 010d	CSP 011	CSP 012	CL 02-21	CL 04-21	
LOI (%)	1.98	1.80	3.47	2.16	5.72	2.11	2.13	1.19	0.53	0.70	1.18	4.05	9.60	
major elements														
XRF (wt%)														
SiO ₂	50.11	55.45	49.59	54.47	51.65	50.97	51.36	52.03	51.72	50.32	50.80	52.90	51.10	
Al ₂ O ₃	16.36	15.14	15.72	15.82	14.53	14.93	14.21	15.86	13.97	15.81	14.57	15.98	14.96	
TiO ₂	1.34	1.46	1.67	1.09	1.06	2.15	2.44	1.21	1.97	1.22	2.21	1.42	0.91	
FeO*	9.69	9.86	12.87	11.11	10.51	12.96	14.48	10.51	13.65	10.28	14.22	10.30	10.22	
MnO	0.16	0.25	0.22	0.20	0.23	±0.26	±0.26	0.22	0.24	0.19	±0.26	0.21	0.21	
CaO	12.25	7.95	8.92	7.63	8.22	8.29	7.96	9.22	9.75	12.28	7.76	9.38	8.76	
MgO	7.81	5.91	7.07	5.16	11.05	5.97	5.09	6.96	5.63	7.24	5.18	6.26	10.67	
K ₂ O	0.20	0.44	0.44	1.41	0.53	0.66	0.24	0.91	0.35	0.33	0.59	0.19	1.80	
Na ₂ O	1.95	3.36	3.34	2.92	2.01	3.59	3.72	2.95	2.54	2.22	4.19	3.20	1.22	
P ₂ O ₅	0.12	0.18	0.15	0.18	0.22	0.23	0.23	0.11	0.17	0.10	0.23	0.15	0.15	
trace elements														
XRF (ppm)														
Ni	83	45	54	17	200	38	13	39	27	53	19	35	146	
Cr	282	134	163	36	640	86	27	103	61	198	34	114	529	
V	275	244	331	292	215	410	±500	281	419	291	484	293	245	
Ga	17	18	21	19	16	23	20	18	23	18	19	20	15	
Cu	82	51	75	43	50	47	42	30	89	73	33	45	61	
Zn	64	83	91	86	95	109	111	67	111	74	92	79	66	
Zr	90	138	110	117	103	136	124	77	117	70	106	92	87	
ICP-MS (ppm)														
La	4.79	10.77	6.25	19.55	20.95	8.21	7.60	6.25	5.82	3.48	6.91	7.43	17.80	
Ce	12.16	24.20	15.57	39.02	45.21	20.67	19.13	13.55	15.14	8.78	17.11	16.95	33.85	
Pr	1.79	3.28	2.25	4.60	5.66	3.08	2.86	1.85	2.27	1.36	2.53	2.33	3.93	
Nd	9.20	15.62	11.58	19.37	24.78	15.97	14.99	9.00	12.29	7.41	13.25	11.33	15.95	
Sm	3.26	5.05	4.17	4.80	5.72	5.58	5.35	3.01	4.55	2.87	4.71	3.56	3.84	
Eu	1.23	1.59	1.66	1.29	1.47	1.93	1.88	1.04	1.62	1.02	1.68	1.33	1.09	
Gd	4.27	6.18	5.45	4.41	4.87	6.98	6.56	3.69	6.01	3.73	5.95	4.53	3.54	
Tb	0.82	1.14	1.03	0.73	0.71	1.28	1.21	0.69	1.15	0.74	1.08	0.81	0.55	
Dy	5.30	7.40	6.65	4.52	3.85	8.25	7.89	4.50	7.52	4.92	7.05	5.22	3.29	
Ho	1.12	1.57	1.42	0.94	0.69	1.77	1.66	0.96	1.65	1.07	1.50	1.10	0.66	
Er	3.10	4.45	3.99	2.55	1.79	4.76	4.60	2.59	4.55	2.91	4.13	2.99	1.74	
Tm	0.44	0.64	0.59	0.38	0.24	0.71	0.67	0.38	0.66	0.42	0.60	0.43	0.24	
Yb	2.76	4.02	3.62	2.36	1.48	4.44	4.13	2.43	4.23	2.70	3.75	2.69	1.55	
Lu	0.43	0.61	0.56	0.37	0.23	0.69	0.63	0.37	0.66	0.42	0.58	0.41	0.23	
Ba	33.00	73.00	110.00	304.66	99.47	93.35	46.88	115.38	34.20	35.53	98.26	67.00	534.00	
Th	0.79	2.37	1.04	4.91	5.19	1.12	1.08	1.17	0.85	0.38	0.99	1.33	4.48	
Nb	2.78	5.42	3.60	5.27	7.94	2.23	2.10	3.17	3.31	1.86	2.07	3.81	2.52	
Y	29.34	41.50	37.86	24.97	18.66	46.60	43.50	24.88	43.59	27.82	39.00	28.16	16.98	
Hf	2.39	3.87	3.09	2.98	2.67	3.66	3.37	2.15	3.26	1.96	2.81	2.45	2.10	
Ta	0.20	0.38	0.26	0.36	0.56	0.15	0.14	0.22	0.25	0.13	0.15	0.27	0.15	
U	0.20	0.68	0.26	0.96	1.03	0.24	0.23	0.29	0.24	0.12	0.20	0.30	0.76	
Pb	1.14	3.61	0.76	4.64	6.09	3.26	4.72	2.38	1.51	1.66	4.76	7.83	4.23	
Rb	5.70	12.90	13.30	32.62	25.67	13.76	5.34	24.16	5.34	3.97	11.48	4.30	66.20	
Cs	1.05	1.23	0.63	2.42	1.73	1.03	0.28	1.84	0.23	0.33	1.13	0.79	6.09	
Sr	164.00	184.00	231.00	321.10	149.77	161.60	180.21	165.10	120.25	113.04	173.95	265.00	114.00	
Sc	45.80	39.90	49.60	37.94	35.08	43.87	47.53	46.11	46.55	48.93	46.22	41.00	42.30	

* total Fe

† value greater than 120% of highest standard

Table 1. Geochemical data for samples obtained for this study.

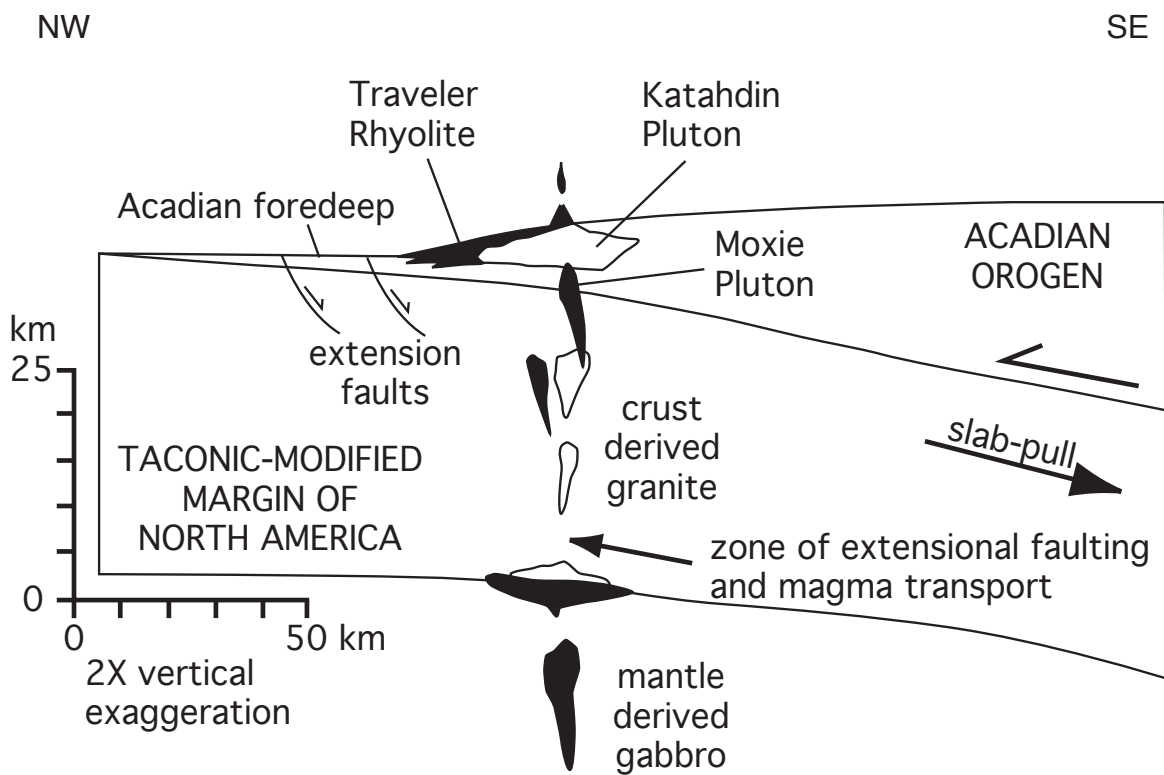


Figure 1. Schematic cross-section of Chesuncook Dome/Katahdin area showing relationship of mafic/granitic magmas to upper and lower plates of Acadian Orogen. Modified from Bradley and Tucker, 2002

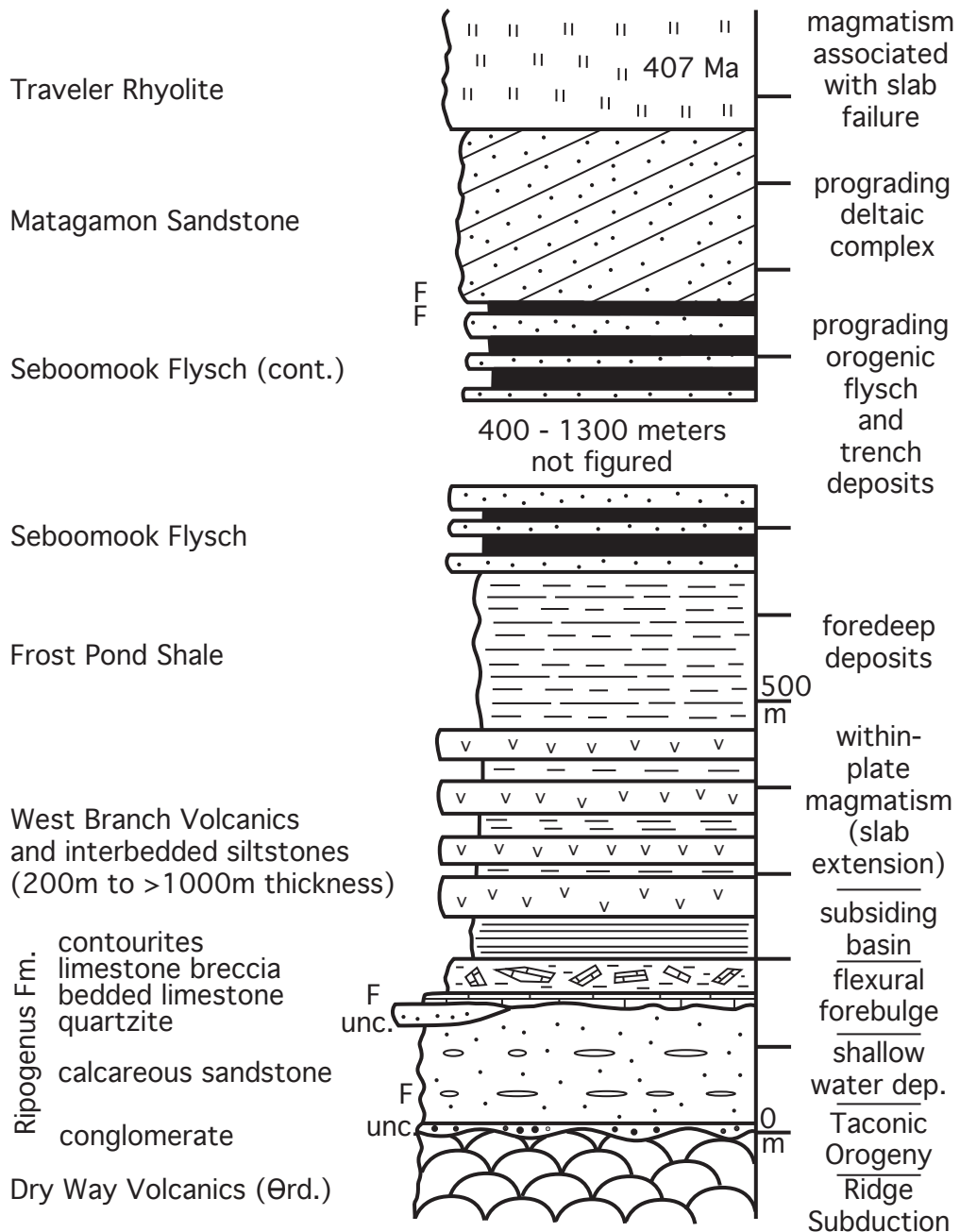


Figure 2. Siluro-Devonian stratigraphic section from the Chesuncook Dome, Ripogenus Dam area. Thicknesses are approximate and may vary. Bedded limestone of Ripogenus Formation exaggerated for clarity. Based on geology of Griscom (1976) and Begeal et al. (2004). F=fossil, unc.=unconformity.

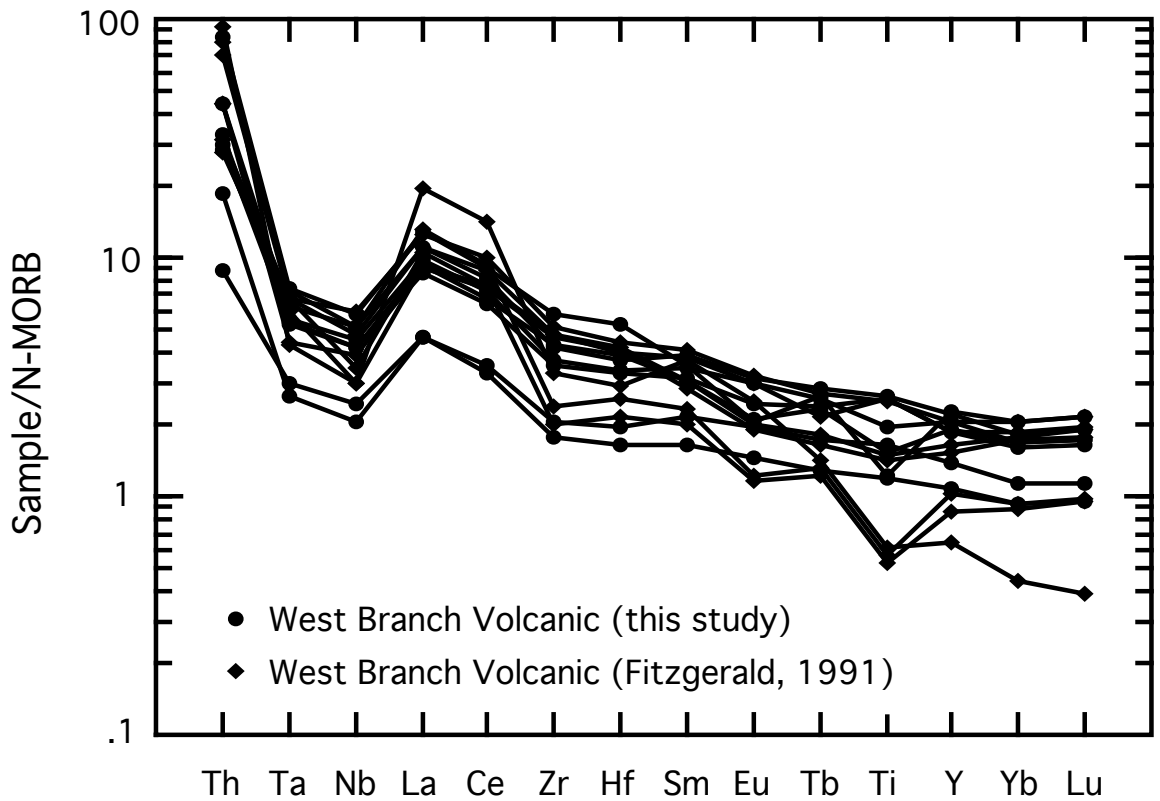


Figure 3. MORB normalized spider diagram of West Branch Volcanics. Normalization values from Sun and McDonough (1989).

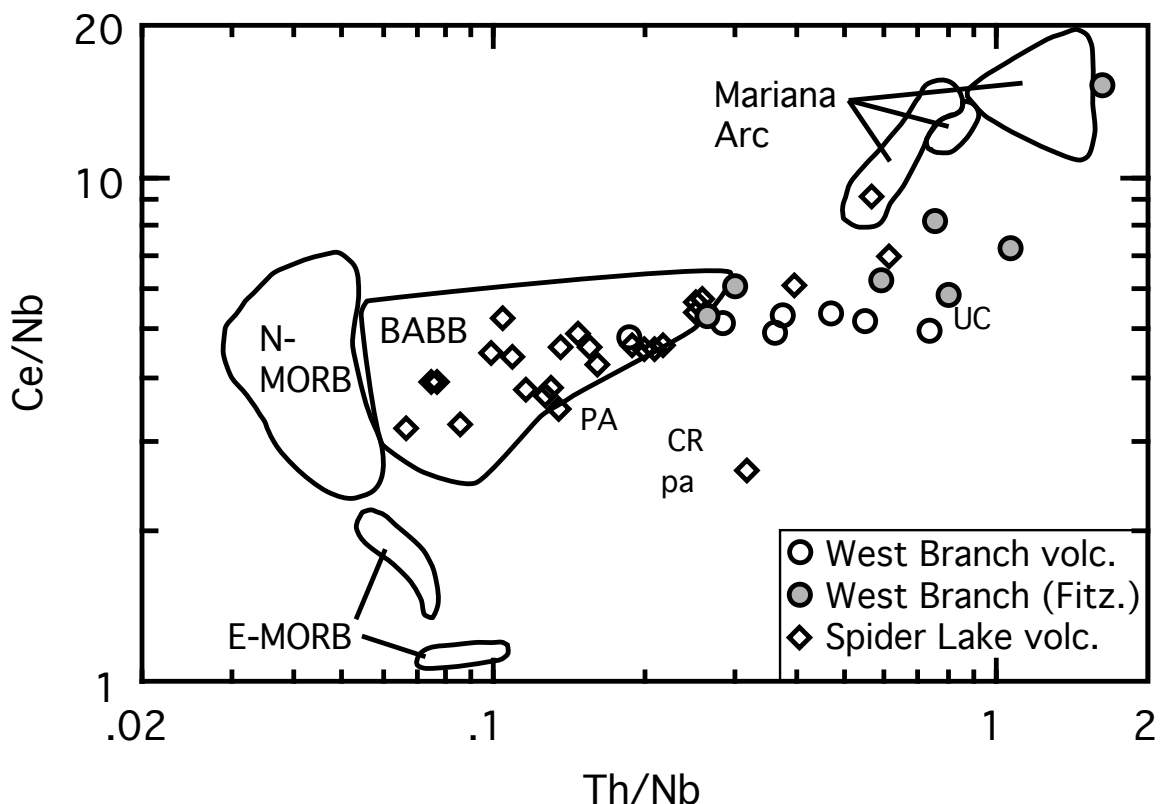


Figure 4. Th/Nb vs. Ce/Nb modified from Saunders and Tarney (1991). UC = upper crustal composition (McLennan, 2001); CR=Columbia River Flood Basalt 27 PHGR-48 R2 (Hooper and Hawkesworth, 1993); PA=Hi-Ti Parana basalt CB-1110 (in Peate, 1997); pa=low-Ti Parana basalt DUP-30 (in Peate, 1997); BABB = back-arc basin basalt. West Branch (Fitz.) and Spider Lake samples from Fitzgerald (1991).

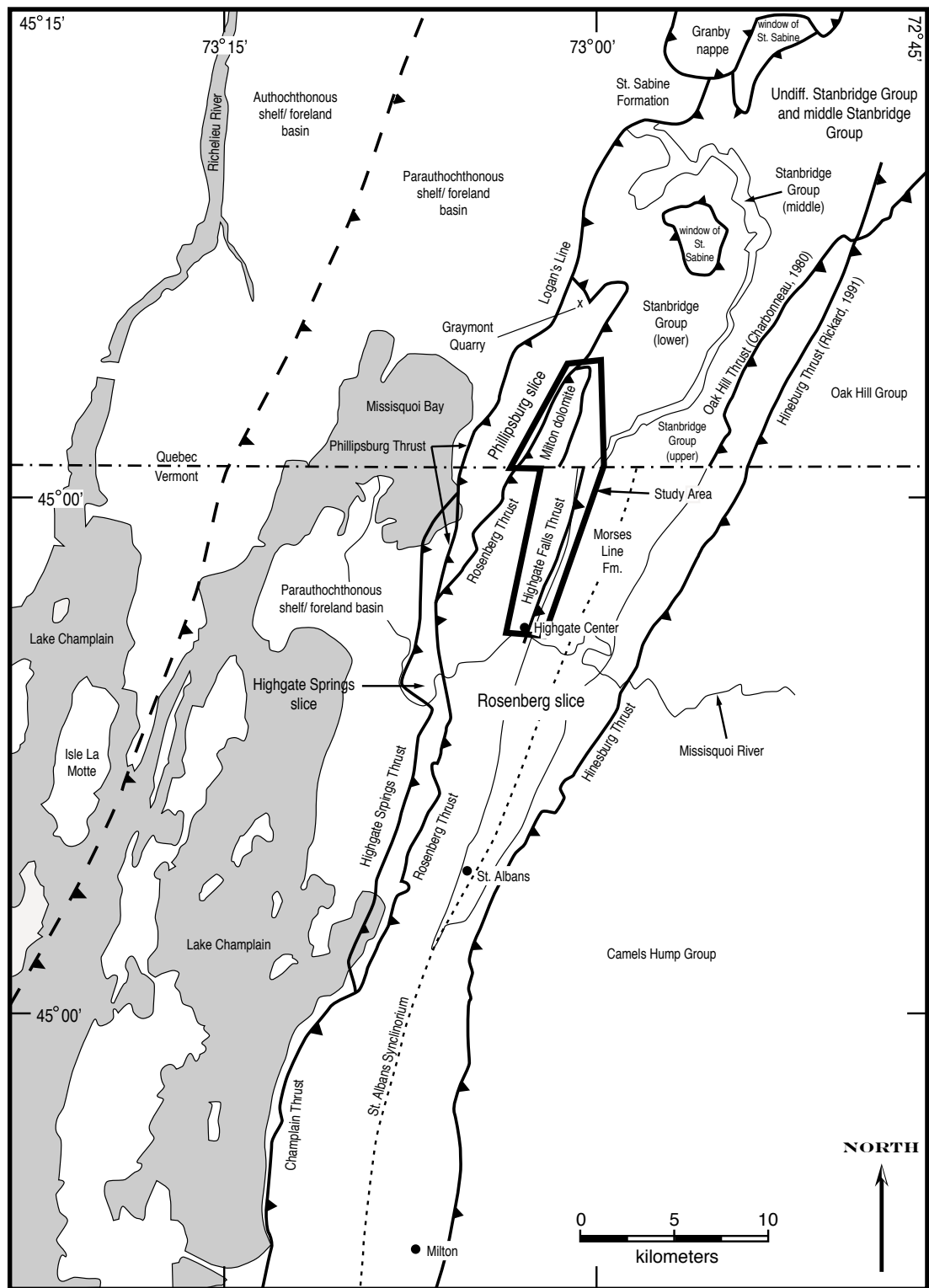


Figure 1. Regional map showing significant structures and lithologic units in the northwestern Vermont and southern Quebec. Based on Doll et al. (1961), Fisher (1968), Charbonneau (1980), Globensky (1981), and Avramtchev (1989). Thrust separating autochthonous and parauthochthonous shelves inferred from local geology.

Figure 2. Lithostratigraphic correlation chart of the Cambrian through Middle Ordovician formations of the Rosenberg slice. Heavy dotted line indicates Cambrian-Ordovician boundary. Light dashed lines indicate members of formations. The several members (St. Albans Slate – Hungerford Slate) of Doll et al. (1961) are part of the Sweetsburg Formation. * Keith (1923) mistakenly correlated the Ordovician limestone conglomerate (Corliss) with the Cambrian Rockledge Conglomerate, which led to correlating the Highgate Slate in the Missisquoi River gorge with the Skeels Corners slate. ** Schuchert (1937) mistakenly assumed the Hungerford Slate lies depositionally below the Rockledge Conglomerate. *** Mehrrens and Dorsey (1987) assigned the name Rockledge to both the Cambrian limestone conglomerates and the lithologically similar Corliss outcrops of Ordovician age.

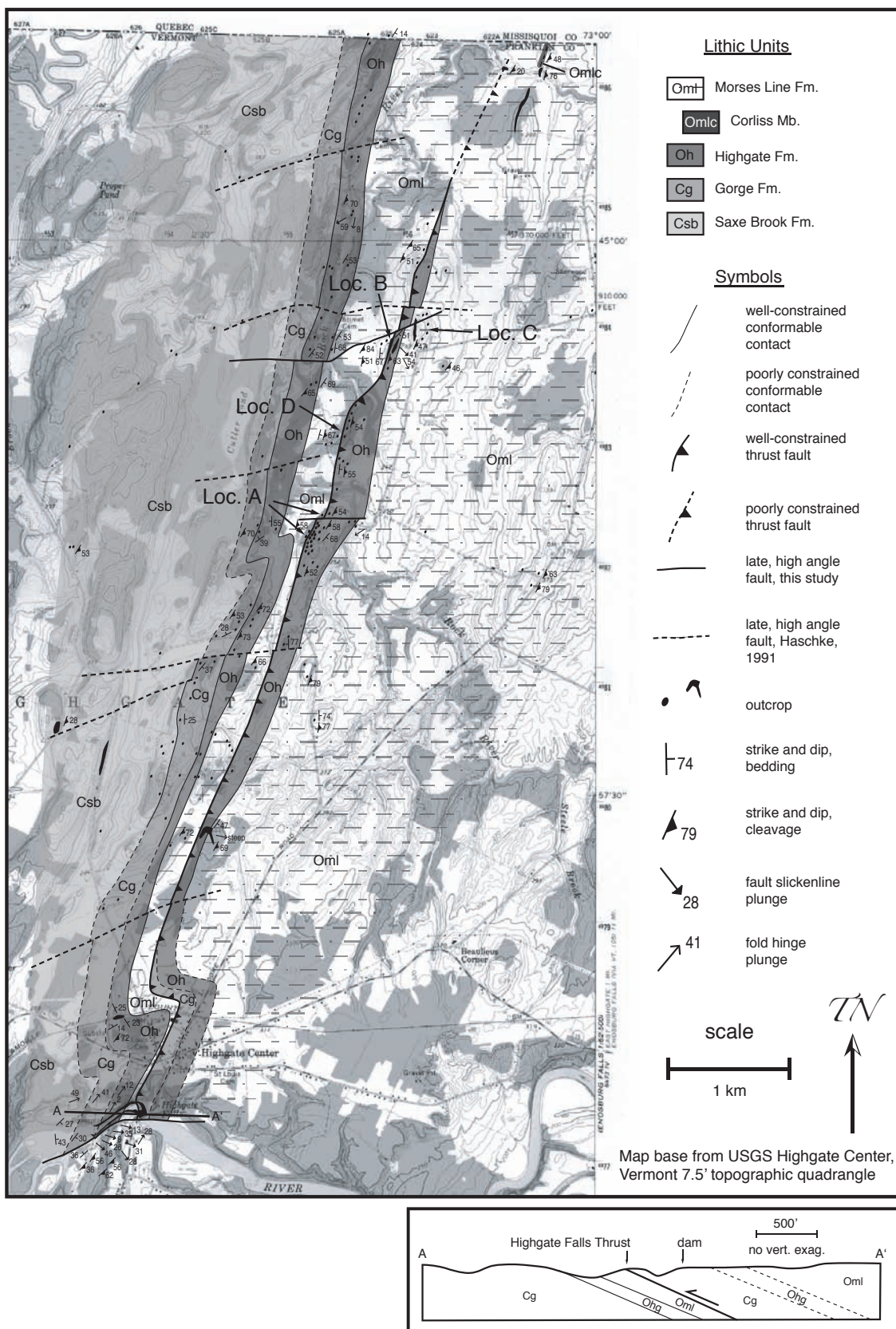


Figure 3. Geologic map of the area between Highgate Center and the International Border, northwestern Vermont.

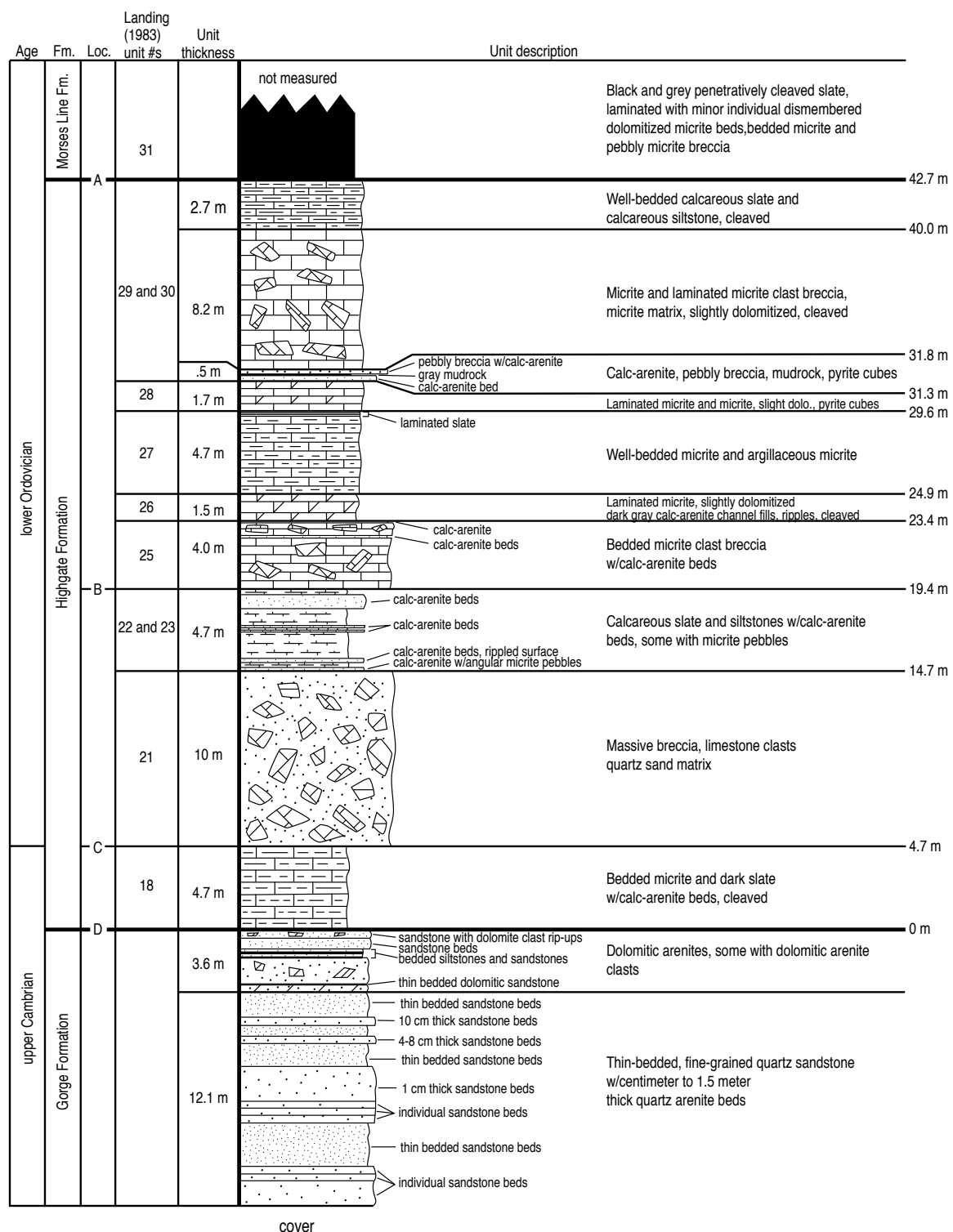


Figure 4. Measured lithostratigraphic section of the exposed units on the north shore of the Missisquoi River gorge at Highgate Center. Locations are keyed to references in the text. Measured section does not include the bulk of the Morse Line Formation, Highgate Falls thrust or upper block of Highgate Falls thrust.



Figure 5. Contact between the Highgate (above) and Gorge (below) Formations in the Missisquoi River gorge at Highgate Center (Loc. D, Figure 7). The large black arrow indicates the contact between the lowest bedded micrite and slate of the Highgate Formation and the uppermost sandstone bed of the Gorge Formation. Small arrow points to small 15 cm tall notebook, slightly oblique to view.

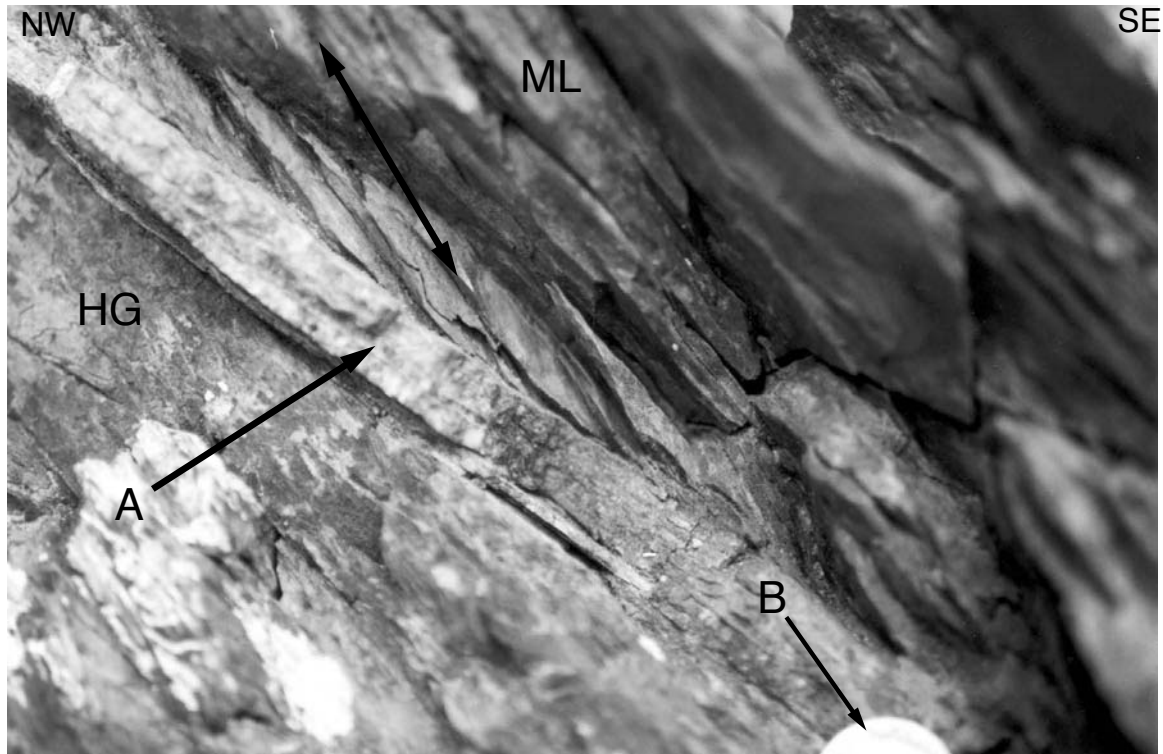


Figure 6. Minor thrust fault at contact between Highgate and Morses Line Formations. Large uni-direction arrow (A) indicates calcite slickenfiber vein, approximately 1 cm thick. Small arrow (B) points to dime for scale, only partially shown. Large bi-directional arrow indicates cleavage orientation. NW = northwest, SE = southeast.

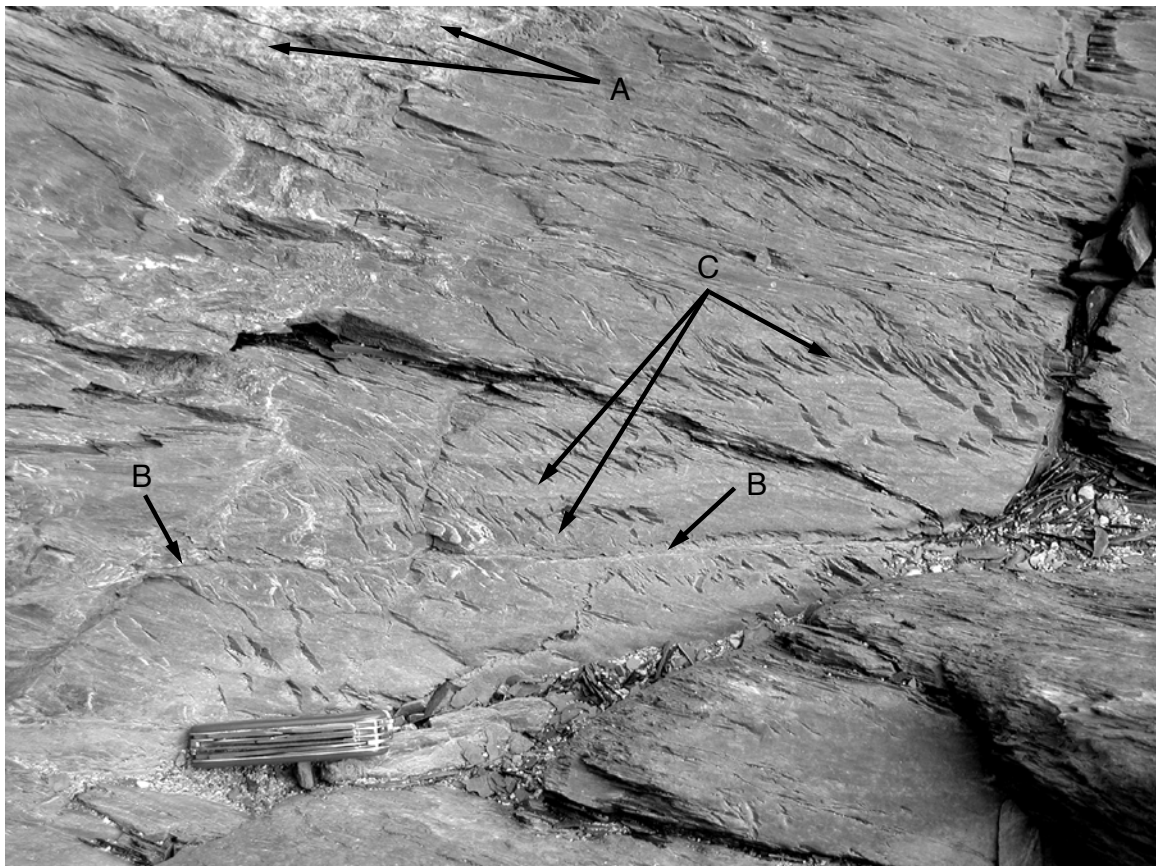


Figure 7. Minor thrust faults and en echelon fractures in Morses Line Formation, Missisquoi River gorge. Arrow A points to deformed fault, slip surface parallels ground surface in photo. B arrows indicated relatively undeformed planar thrust that cuts oblique to ground surface. Both faults are surrounded by extension fractures (C arrows), although those associated with the deformed fault do not show original en echelon arrangement. Pocketknife for scale is 9 cm long.



Figure 8. Folded minor thrust in Morses Line Formation of Missisquoi River gorge. Uni-directional arrow points to folded, annealed calcite slickenfiber vein. 14 cm long pencil is oriented approximately with average fault orientation. Bi-direction arrow indicates cleavage orientation.



Figure 9. Dismembered dolomitic micrite beds in slates of Morses Line Formation (large arrows). Small arrow (A) is 19 cm high field notebook.

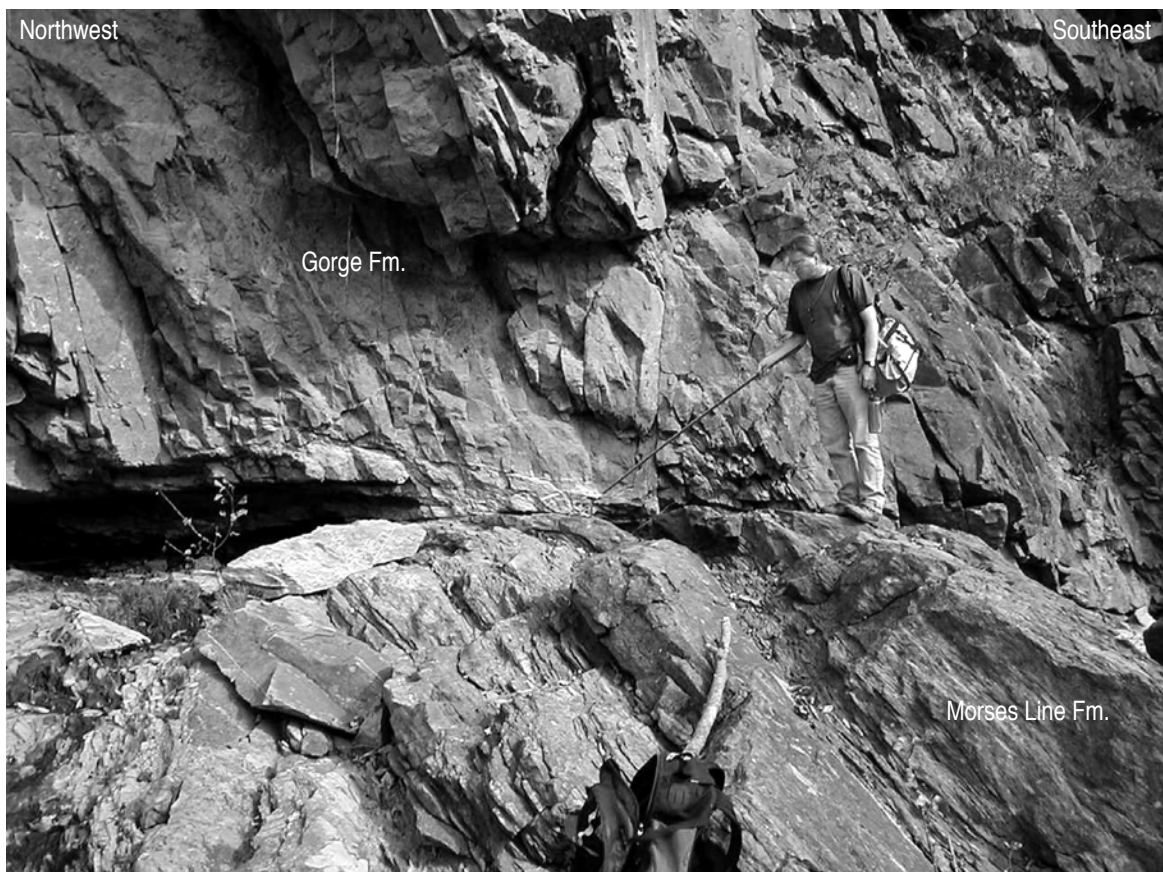


Figure 10. Highgate Falls thrust exposed in the Missisquoi River Gorge. Author is using pointer to indicate slip surface. Upper block has moved to the left in photo. Photo courtesy of Marjorie Gale.

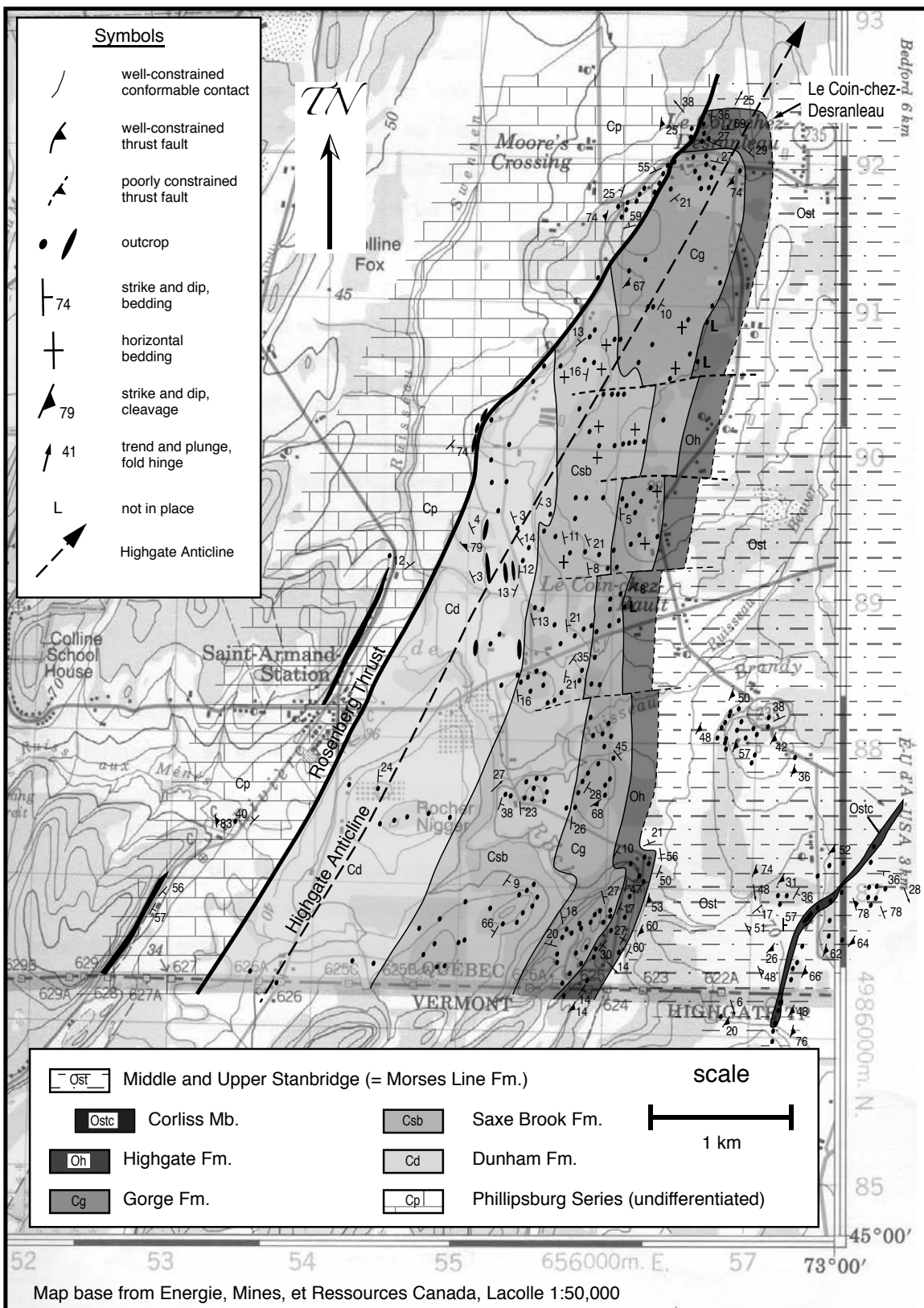


Figure 11. Geologic map of the area from Le Coin-chez-Desranleau to the International Border, southern Quebec.

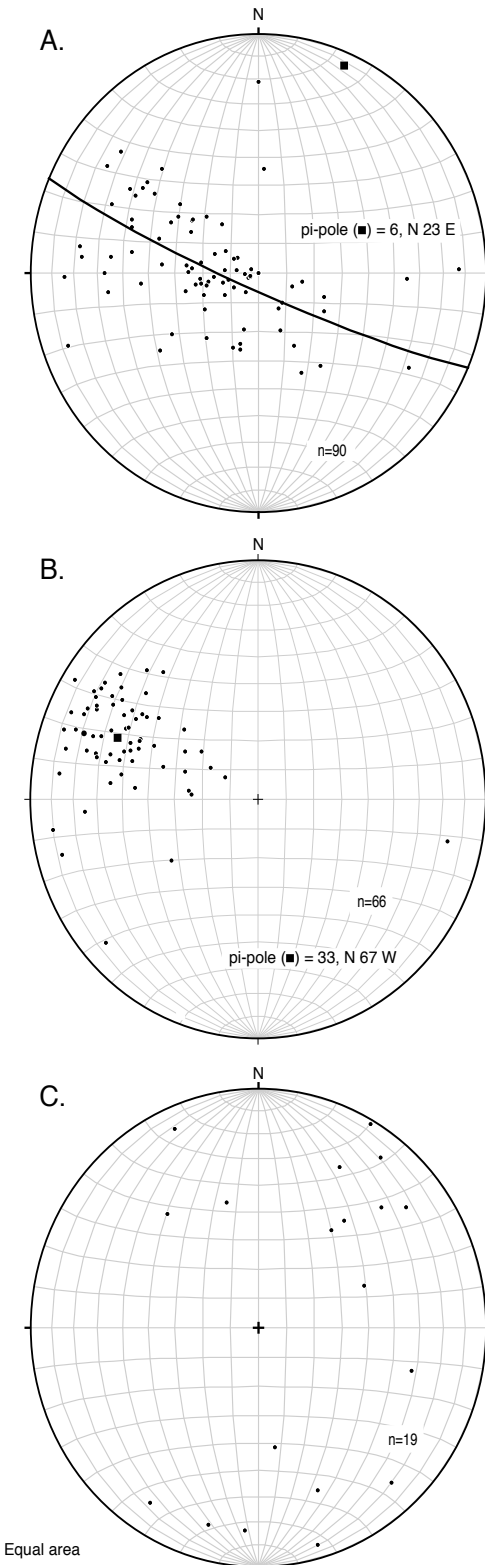


Figure 12. Stereonet representations of structural data from both Vermont and Quebec field areas. A) poles to bedding; B) poles to penetrative cleavage; C) fold hinges, including some late fold hinges.